Electronic Supplementary Material (ESI) for MedChemComm.

Supplementary material

Radioligand binding assays

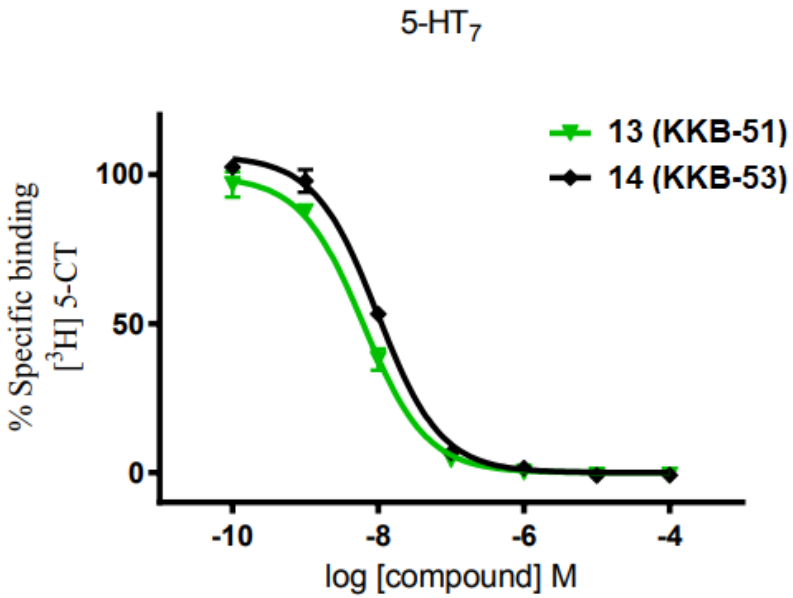

	KKB-51	KKB-53
One site competition		
Best-fit values		
Bottom	= 0	= 0
Top	99.47	120.5
LogEC50	-8.202	-8.153
EC50	6.282e-009	7.037e-009
KI	3.065e-009	3.432e-009
Ligand (Constant)	0.84	0.84
Kd (Constant)	0.8	0.8
Std. Error		
Top	1.782	6.203
LogEC50	0.03917	0.1132
95% CI (asymptotic)		
Top	95.58 to 103.3	107 to 134
LogEC50	-8.287 to -8.117	-8.399 to -7.906
EC50	5.161e-009 to 7.647e-009	3.988e-009 to 1.241e-008
KI	2.518e-009 to 3.73e-009	1.946e-009 to 6.056e-009

Scheme S1. Example binding curves for the two of the most active compounds **13** and **14**

Table S1. Radioligand binding results for compounds **1**-**18** ; K_i values with SD.

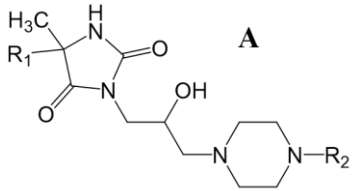

A

1-15

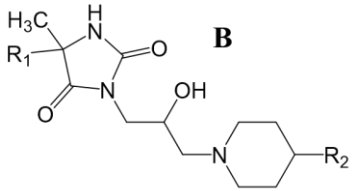

B

16, 17

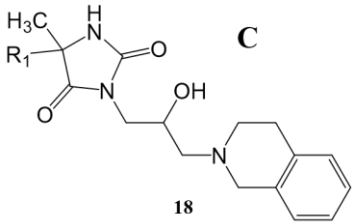

C

18

Cpd	Group	R^1	R^2	K_i [nM]		
				D_2R^1	5-$HT_{1A}R^2$	5-HT_7R^3
1[*]	A	4-Fluorophenyl	2-MeO-phenyl	715 ± 48	121 ± 8	3 ± 1
2[*]	A	4-Fluorophenyl	Benzhydryl	261 ± 31	5570 ± 749	79 ± 6
3[*]	A	4-Fluorophenyl	Phenyl	2906 ± 362	2733 ± 196	223 ± 35
4	A	4-Fluorophenyl	Benzyl	20030 ± 1767	377500 ± 2547	2085 ± 167
5	A	4-Fluorophenyl	Benzoyl	10080 ± 719	6216 ± 781	3609 ± 454
6	A	4-Fluorophenyl	(Naphtalene-1-yl)methyl	5233 ± 442	5577 ± 723	2172 ± 322
7	A	4-Fluorophenyl	1-Naphtyl	295 ± 17	19 ± 3	11 ± 2
8	B	4-Fluorophenyl	Phenoxyl	4353 ± 675	5211 ± 691	165 ± 18
9	B	4-Fluorophenyl	4-Cl-Phenoxyl	4116 ± 349	21470 ± 1479	172 ± 15
10	A	1-Naphtyl	2-MeO-Phenyl	256 ± 13	325 ± 41	5 ± 1
11	A	1-Naphtyl	2-CN-Phenyl	416 ± 29	1225 ± 174	19 ± 3
12	A	1-Naphtyl	Benzhydryl	273 ± 37	413200 ± 34297	224 ± 19
13	A	2-Napthyl	2-MeO-Phenyl	153 ± 22	128 ± 11	3 ± 1
14	A	2-Naphtyl	2-CN-Phenyl	264 ± 34	129 ± 18	3 ± 1
15	A	Methyl	2-MeO-Phenyl	2130 ± 307	489 ± 65	125 ± 9
16	A	Methyl	2-CN-Phenyl	3429 ± 451	1155 ± 78	209 ± 36
17	A	Methyl	Benzhydryl	1152 ± 94	15150 ± 1663	824 ± 68
18	C	4-Fluorophenyl	-	5848 ± 714	1551 ± 164	888 ± 91
Ref[a-c]				9[a]	20[b]	18[c]

[*]Compounds from the previously published and pharmacologically described series.[1-3]Radioligands used: [^{3}H]-Raclopride (D_2R), [^{3}H]-8-OH-DPAT (5-$HT_{1A}R$), [^{3}H]-5-CT (5-HT_7R). [a-c]Reference ligands for GPCRs investigated: [a]olanzapine, [b]buspirone, [c]clozapine, nt - not tested.

Table S2. Comparison of radiolignad binding results for basic form and corresponding hydrochloride salts of compounds **10** and **18**

	5-HT$_7$R K_i **[nM]**	
	Basic form	hydrochloride
10	5	7
18	888	843

Metabolic stability results

The metabolic pathways and the most probable structures of metabolites for the 5-HT_7R ligands (**2**, **7**, **10** and **13**) were determined, by using MS and ion fragmentation analyses, supported by predicted *in silico* the most probable sites of metabolism (Fig. S1-S11 and Table S3).

Table S3. Metabolic pathways of the 5-HT_7R ligands after 120 min reaction with MLMs.

Substrate	Molecular mass of substrate (*m/z*)	Amount of metabolites	Molecular mass of the metabolite (*m/z*)	Metabolic pathway
2	517.06	2	423.21 (M1)*	decomposition
7	477.25	4	439.21 (M1)*	oxidation/decomposition
			441.15 (M2)	decomposition
			493.20 (M3)	hydroxylation
			507.22 (M4)	double-hydroxylation/ dehydrogenation
10	489.28	4	505.23 (M1)*	hydroxylation
			383.26 (M2)	decomposition
			475.25 (M3)	demethylation
			505.23 (M4)	hydroxylation
13	489.28	6	505.23 (M1)*	hydroxylation
			383.26 (M2)	decomposition
			305.17 (M3)	decomposition
			475.25 (M4)	demethylation
			505.36 (M5)	hydroxylation
			519.19 (M6)	double-hydroxylation

*main metabolite

The ion fragmentation analysis of the main metabolite of compound **7** (M1) showed several reactions, including hydroxylation, oxidation and decomposition of the naphthyl ring (Table S3, Fig. S1 and S2). Moreover, the hydroxylated, double-hydroxylated and dehydrogenated metabolites of **7** were also observed (Table S3 and Fig. S3). Due to the fact that compounds **10** and **13** possess high structural similarity, the same hydroxylated main metabolite (M1) was observed for both substrates (Table S3, Fig. S4 and S6). The similar reaction of demethylation was also observed (Table S3, Fig. S5 and Fig. S7). However, despite of structural similarity, compound **13** seems to be more susceptible for metabolic bioconversions (table S3, Fig. S6-S9). The higher CL_{int} value of **13** was calculated if comparing to the compound **10** (43.4and 29.0ml/min/kg respectively, Table 3 in the main article), and the presence of two additional metabolites obtained by **13** decomposition or double-hydroxylation was determined (Table S3, Fig. S8 and S9).

Moreover, the most probable metabolic pathway of **2** in the presence of MLMs was identified by obtained MS analysis as a compound decomposition (M1). Regarding the previous studies for **2**, where only slight amount of one dehydrogenated metabolite was found after incubation with human liver microsomes[21], compound **2** seems to be more susceptible for metabolism in mice than in human. Moreover the metabolic pathway of **2** differ between both species (Fig. S10 and S11).

Regarding the metabolic stability, the UPLC spectra after 120 min of incubation with MLMs showed that ~65-70% of compounds **7** and **13** were metabolized into four or six metabolites respectively (Fig.S9), whereas ~40% of compound **10** into four metabolites (Fig. S1-S9, Table S3, see also Table 3 in the main paper). However, the metabolic stability of **10** is the closest to the most stable lead **2** (~20% remaining, metabolized into one metabolite (see Fig. S10 and S11, Table S3 and Table 3 in the main article). For comparison, the UPLC spectra after 120 min reaction of the reference drug aripiprazole with mouse liver microsomes are shown in Fig.S12.

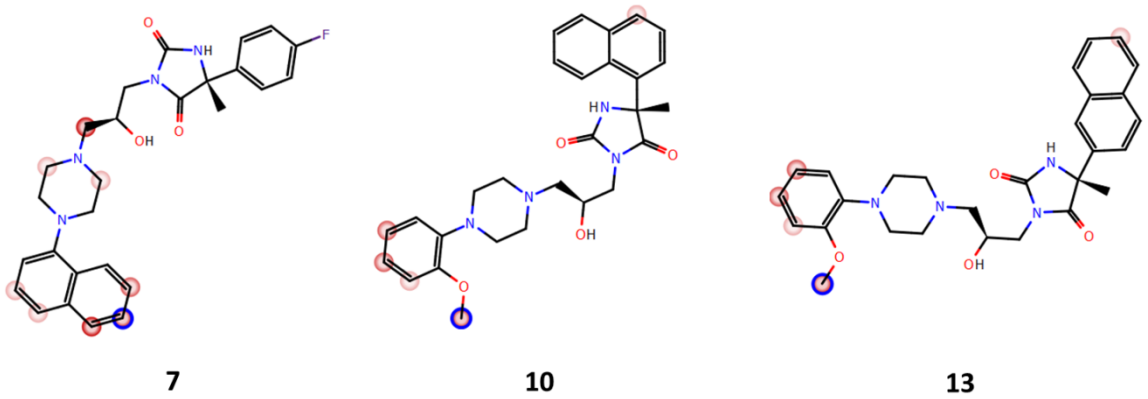

Fig. S1. The *in silico* prediction of the most probably sites of metabolism of **7**, **10**, **13** by using MetaSite 5.1.1 software [1]. The darker red color of the marked functional group indicates its higher probability to be involved in the metabolism pathway. The blue circle marked the site involved in metabolism with the highest probability (100%).

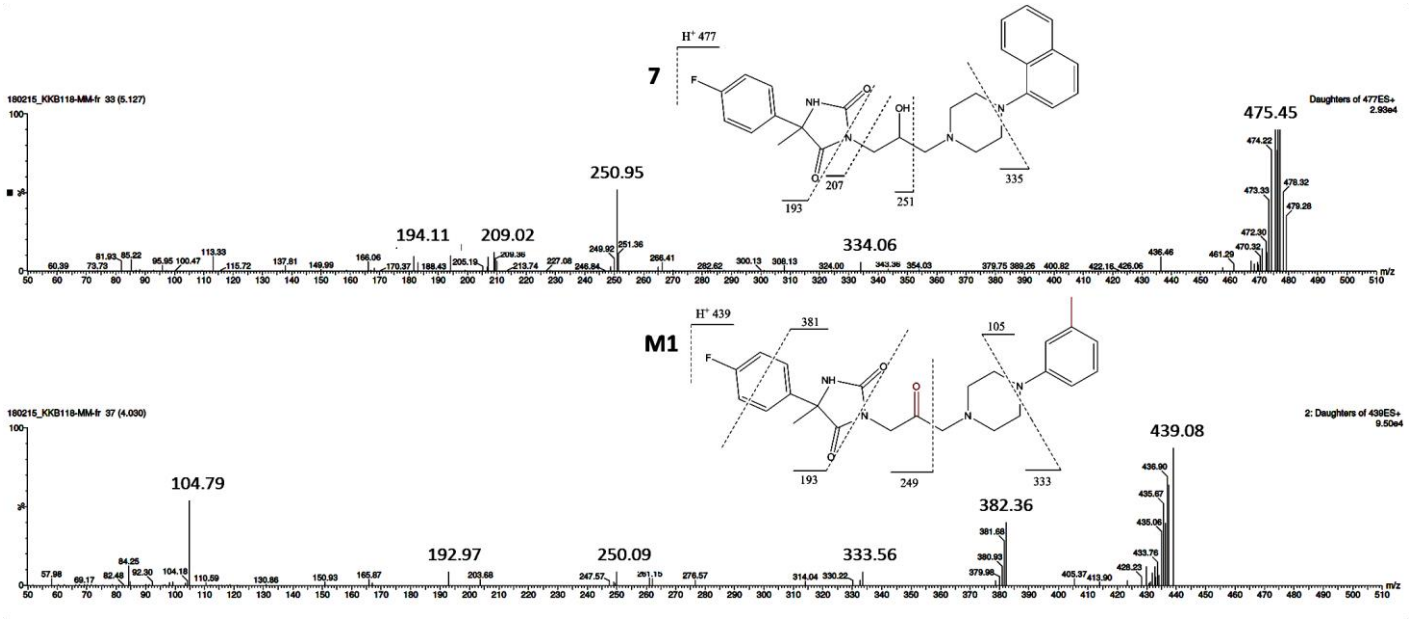

Fig.S2. The MS ion fragmentation analysis of **7** and its main metabolite M1.

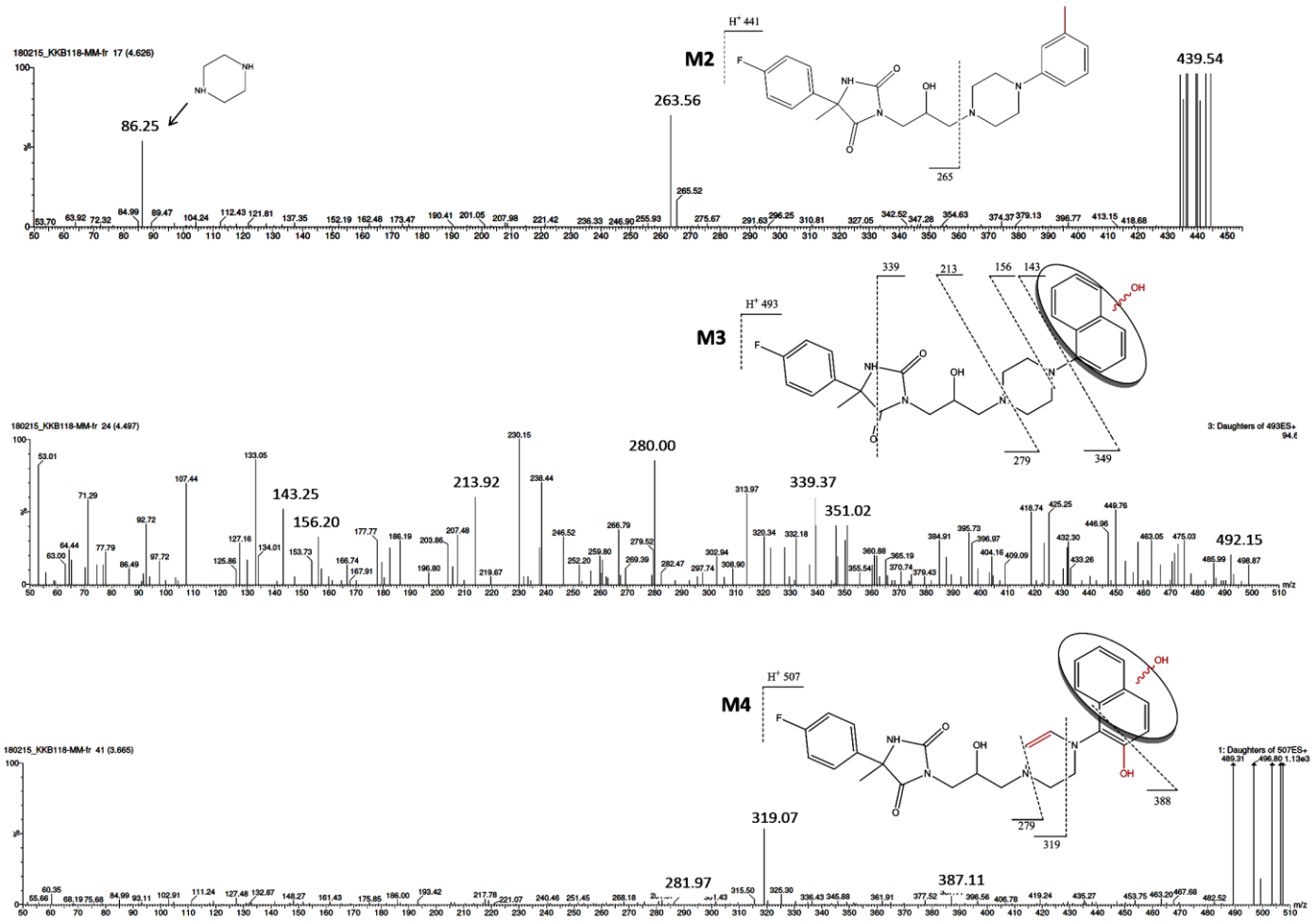

Fig.S3. The MS ion fragmentation analysis of compound's **7** metabolites M2-M4.

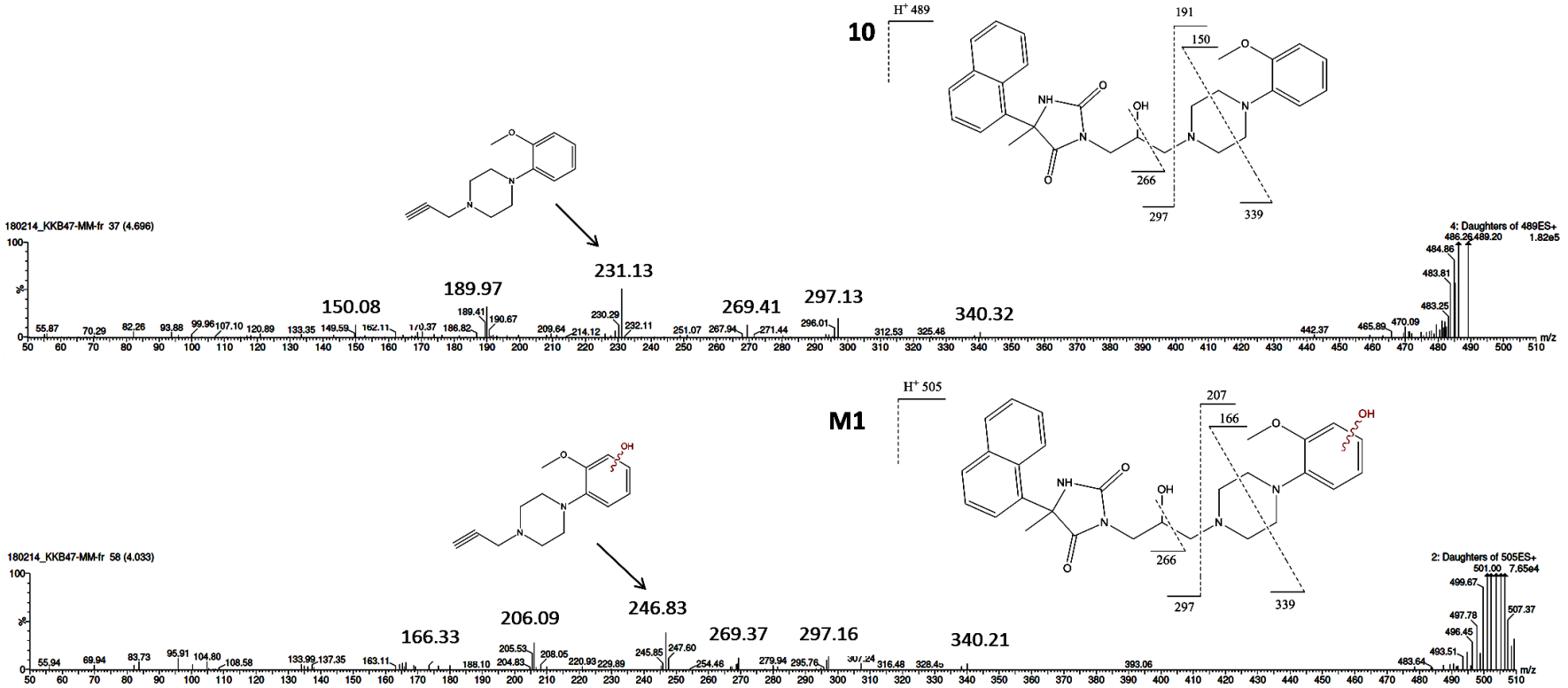

Fig.S4. The MS ion fragmentation analysis of **10** and its main metabolite M1.

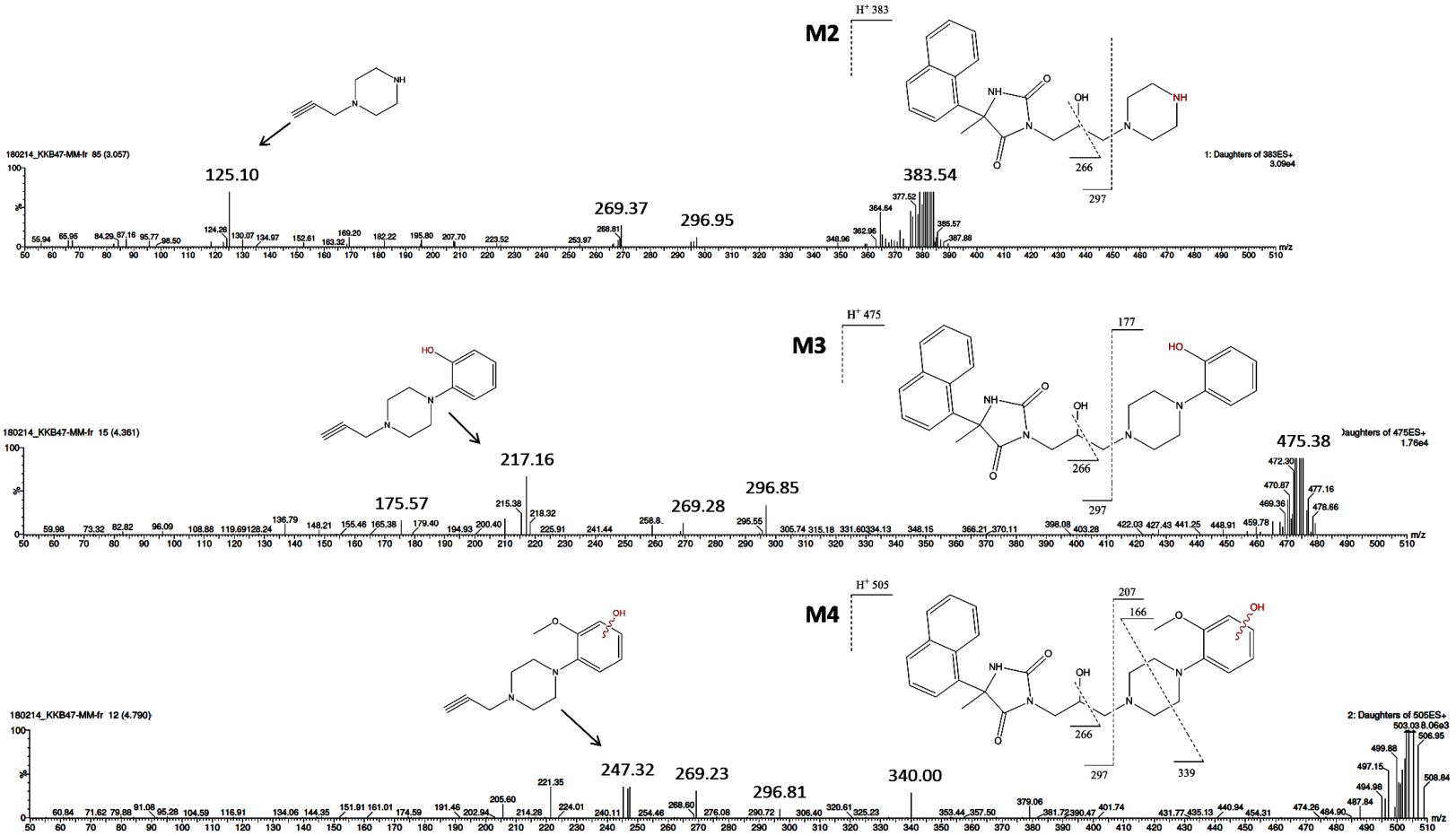

Fig.S5. The MS ion fragmentation analysis of compound's **10** metabolites M2-M4.

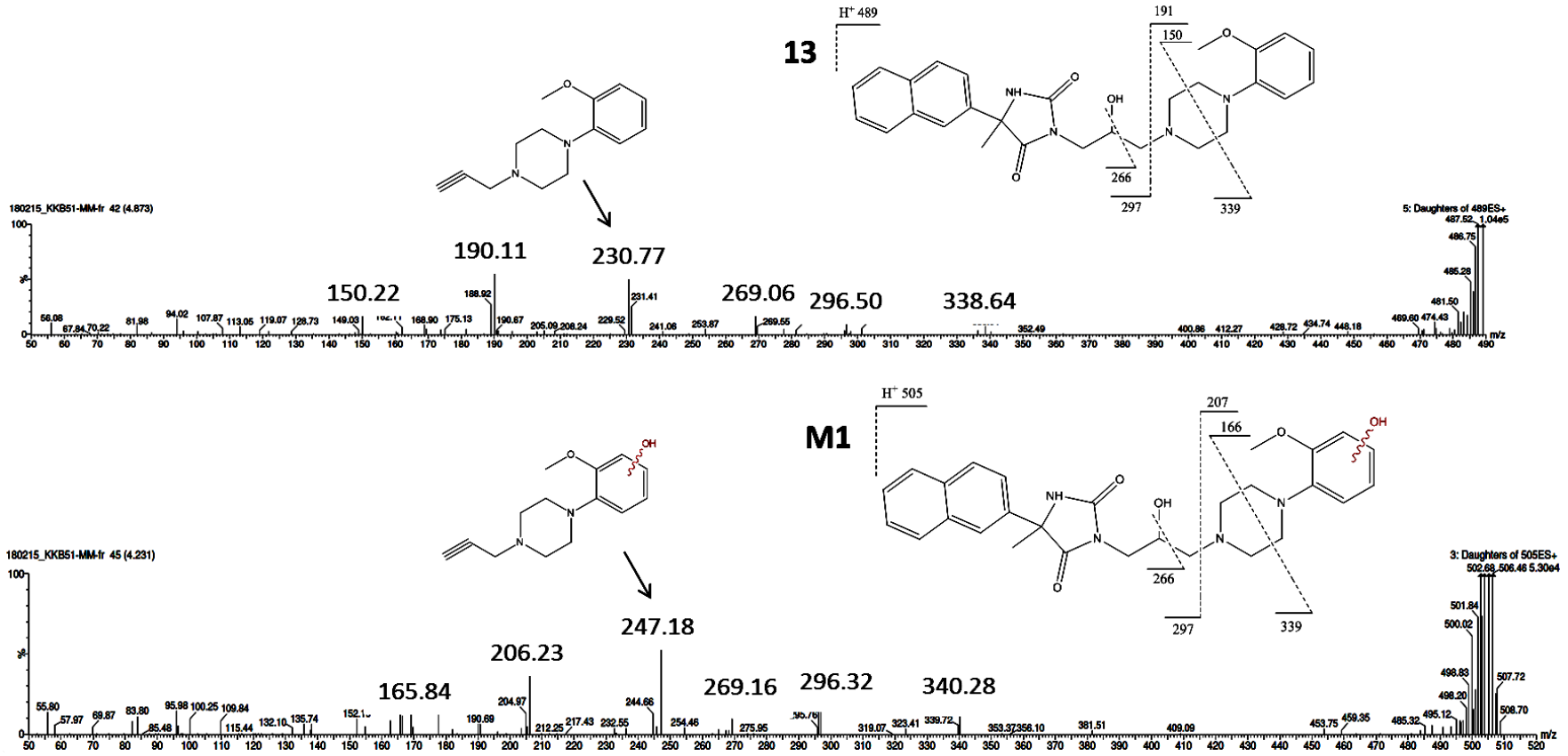

Fig.S6. The MS ion fragmentation analysis of **13** and its main metabolite M1.

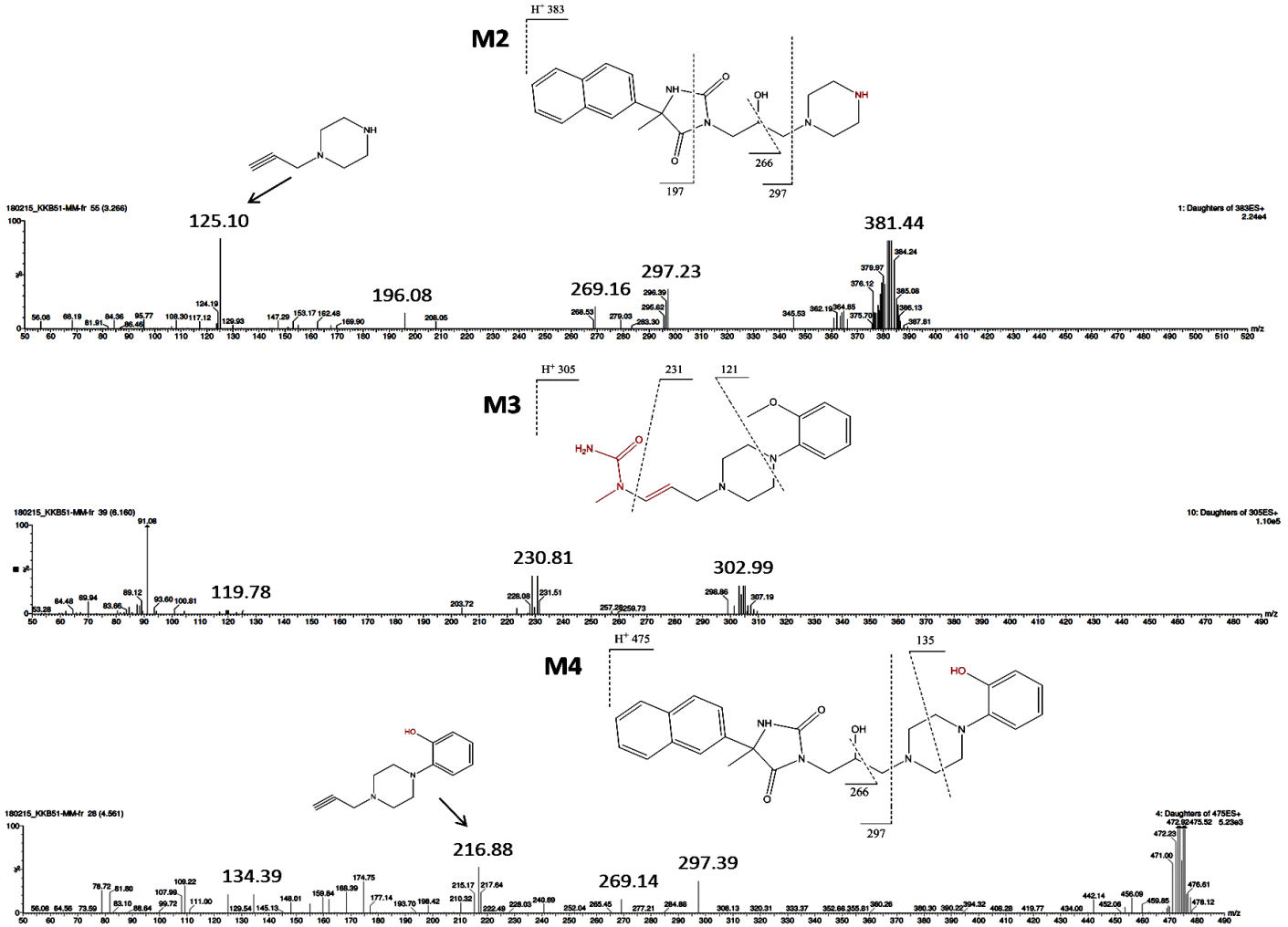

Fig.S7. The MS ion fragmentation analysis of compound's **13** metabolites M2-M4.

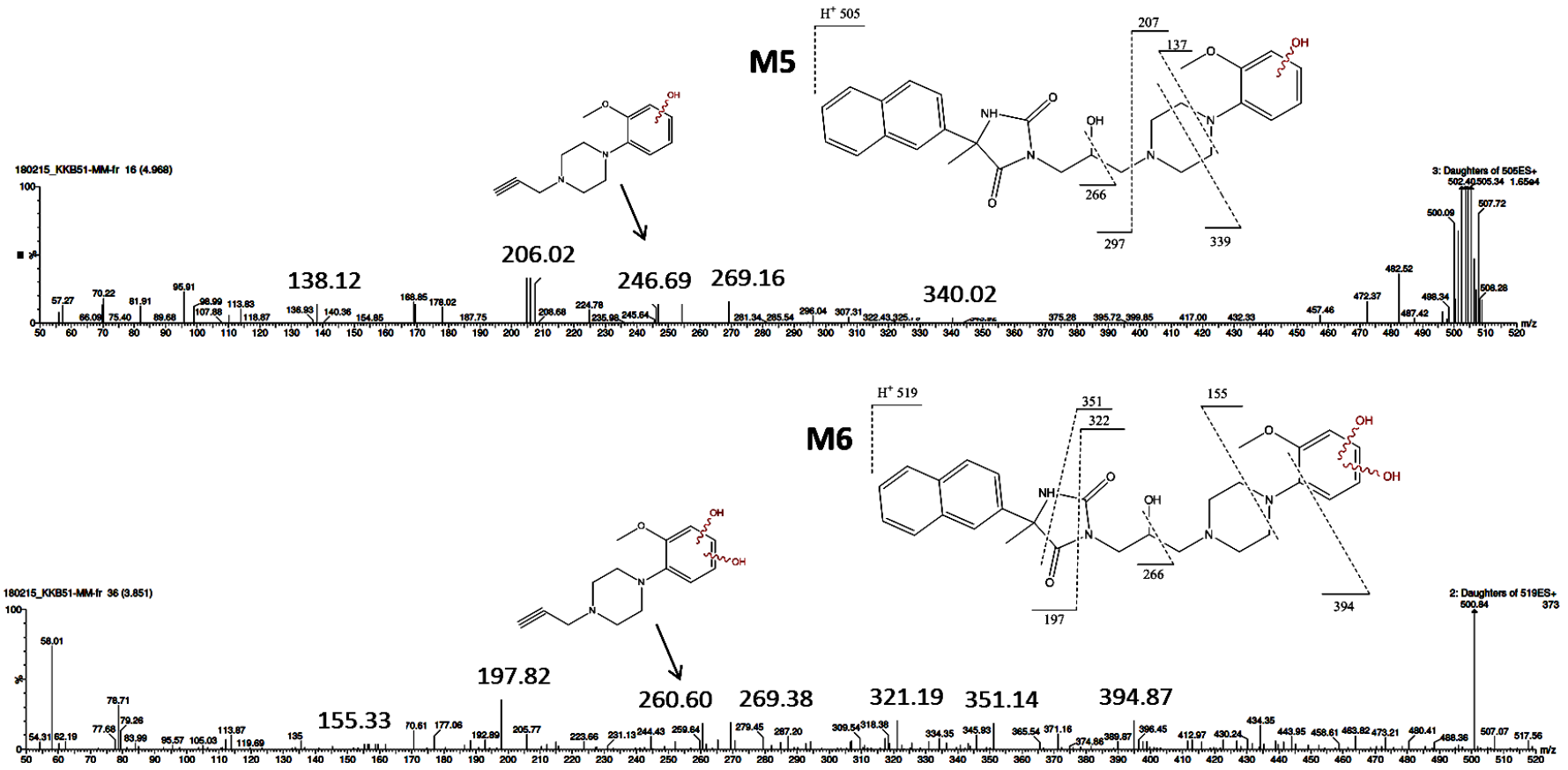

Fig.S8. The MS ion fragmentation analysis of compound's **13** metabolites M5-M6.

Interestingly, each examined compound was converted mostly into the main metabolite (M1), whereas only the trace amounts of other metabolites were found (Fig. S9, A-C).

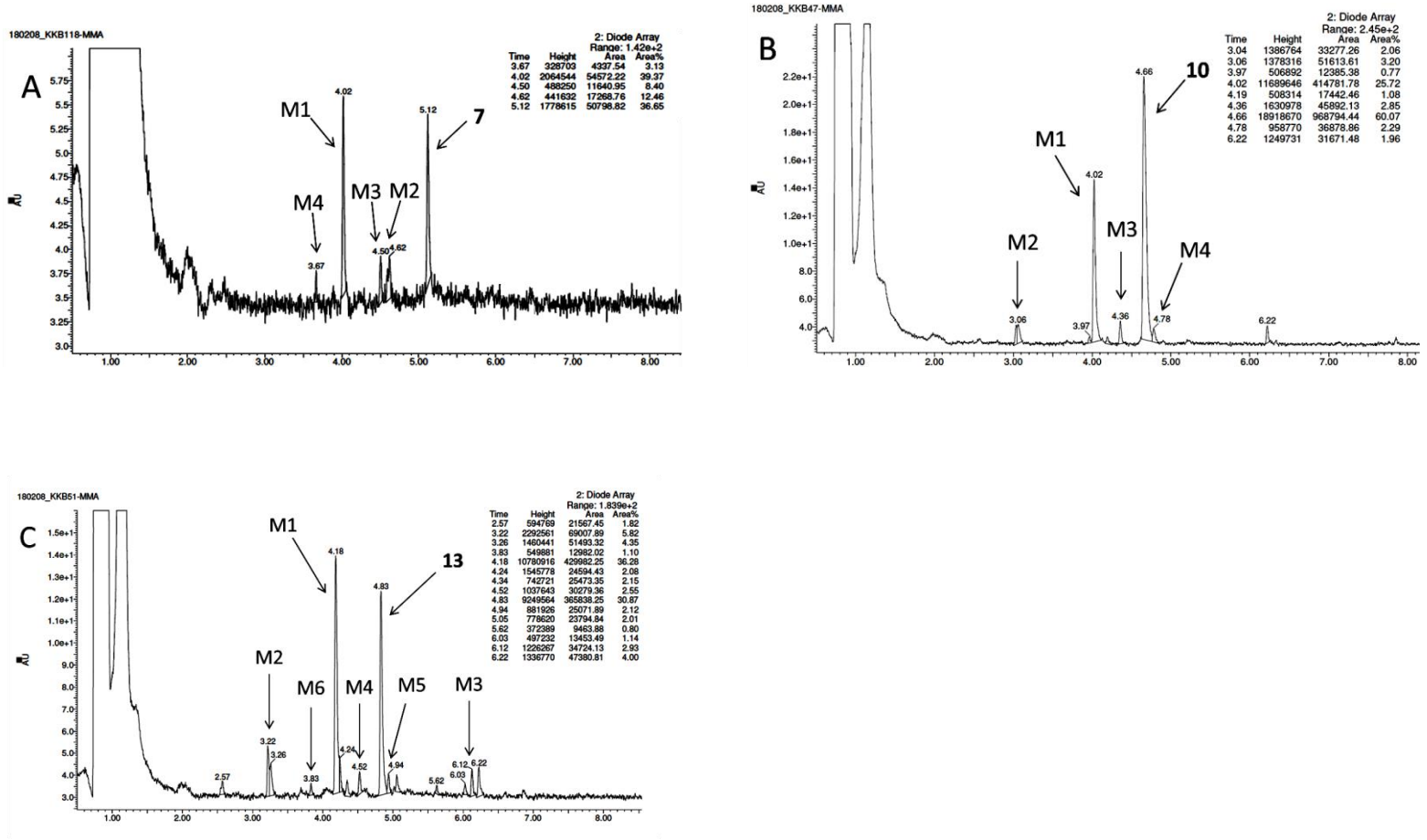

Fig. S9. The UPLC spectra after 120 min reaction of **7** (A), **10** (B), and **13** (C) with MLMs.

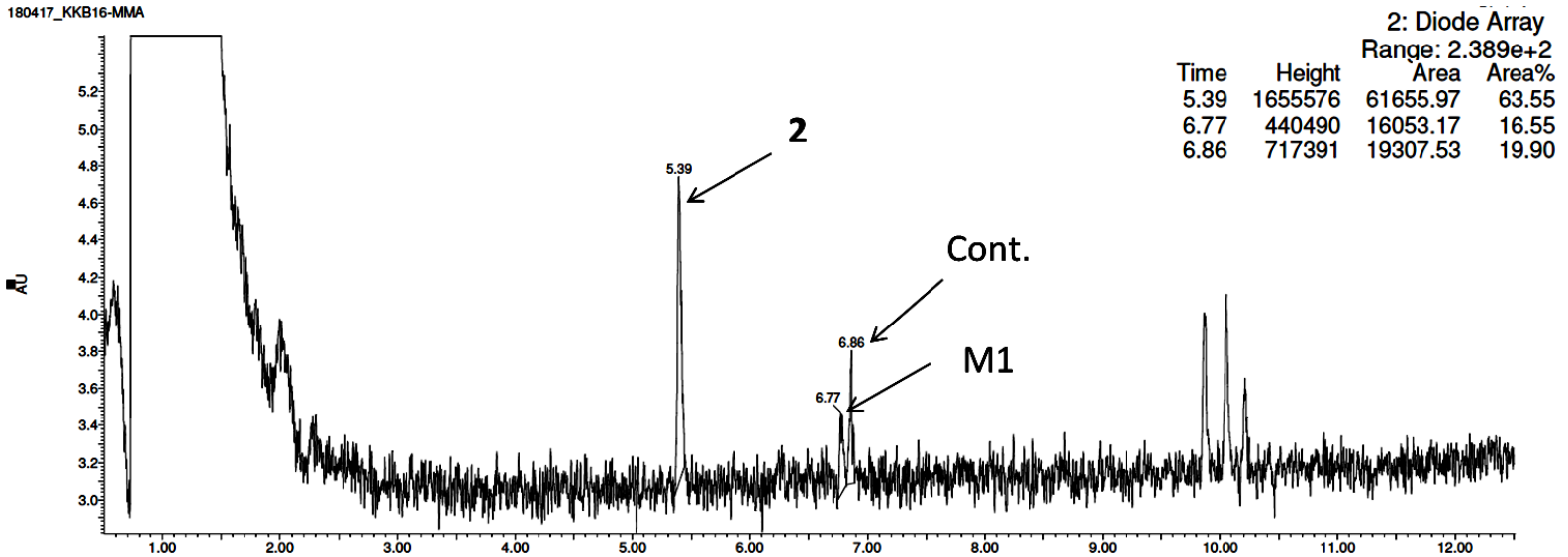

Fig.S10. The UPLC spectra after 120 min reaction of **2** with MLMs. Peak at t_R = 6.86 was identified as contamination. Around 20% of **2** were calculated (excluding contamination) to be metabolized into one metabolite.

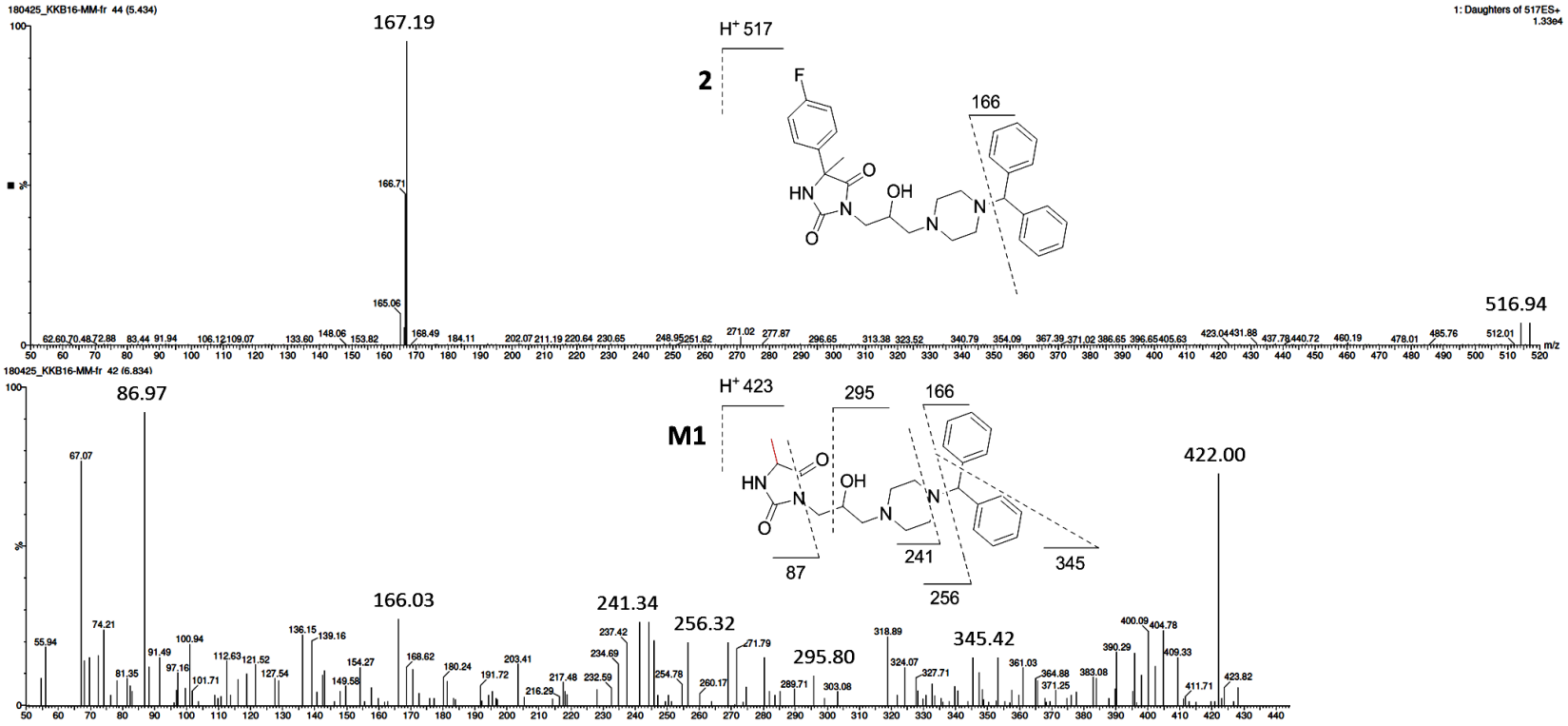

Fig.S11 The MS ion fragmentation analysis of compound **2** and its metabolite M1.

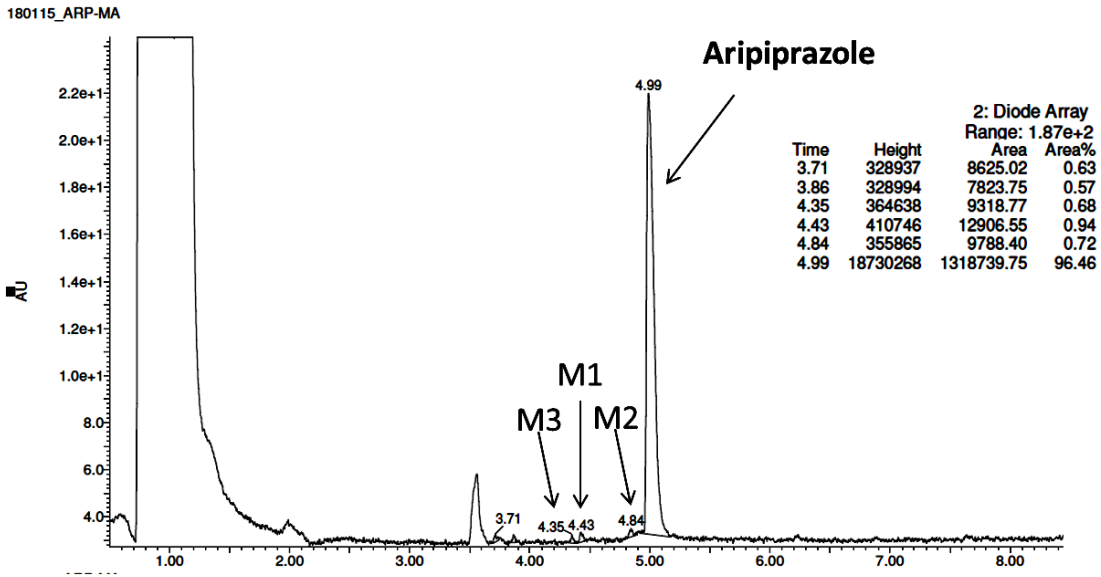

Fig. S12. The UPLC spectra after 120 min reaction of the reference drug aripiprazole with mouse liver microsomes.

References

[1] G. Cruciani, E. Carosati , E. De Boeck, K. Ethirajulu, C. Mackie, T. Howe, R. Vianello. MetaSite: understanding metabolism in human cytochromes from the perspective of the chemist. J Med Chem, 2005, 48, 6970–6979 .

^{1}H NMR and ^{13}C NMR spectra of final compounds and intermediates

3-[3-(4-benzylpiperazin-1-yl)-2-hydroxypropyl]-5-(4-fluorophenyl)-5-methylimidazolidine-2,4-dione **(4)**
^{1}H NMR. 300 MHz. DMSO

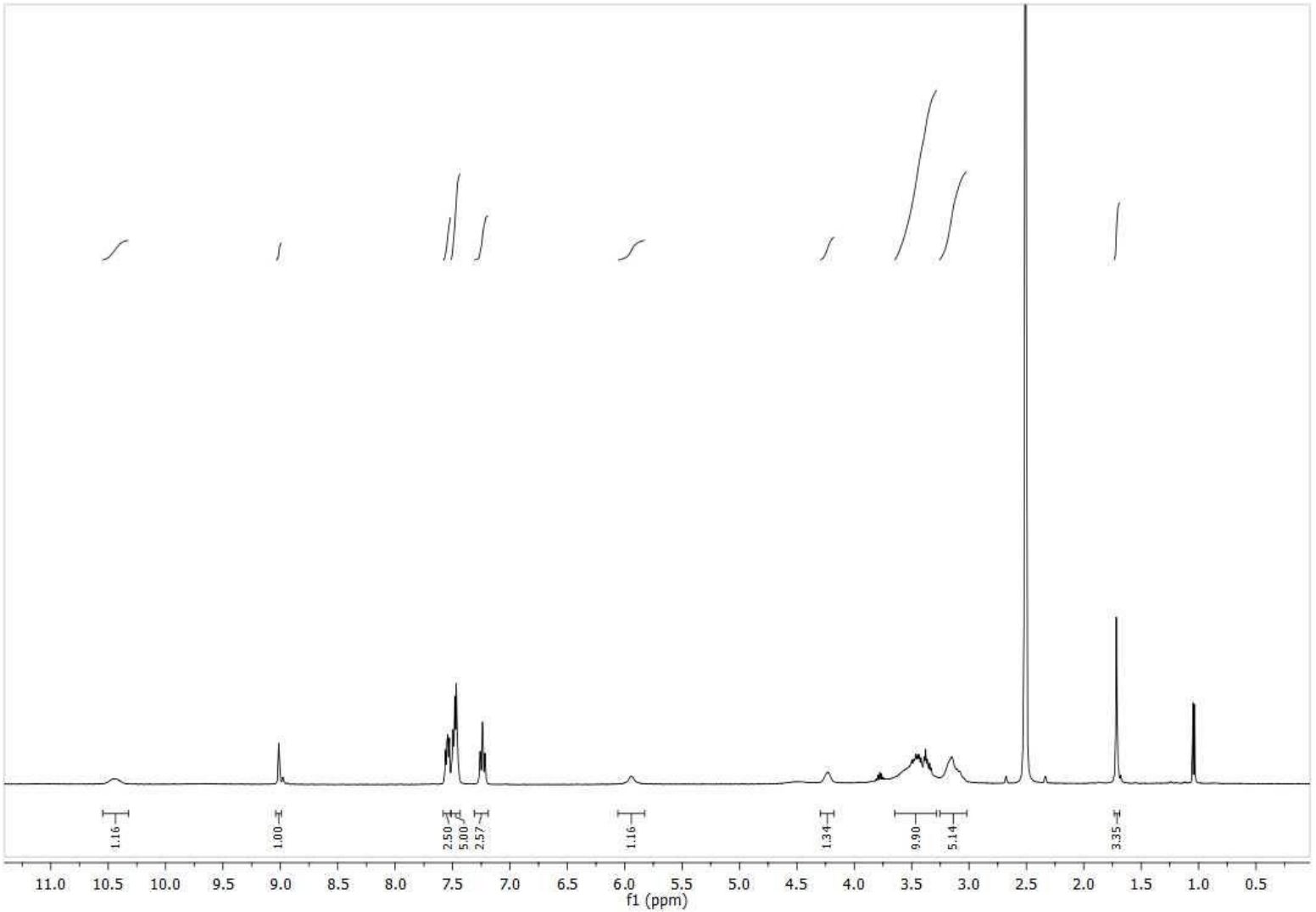

^{13}C NMR. 300 MHz. DMSO

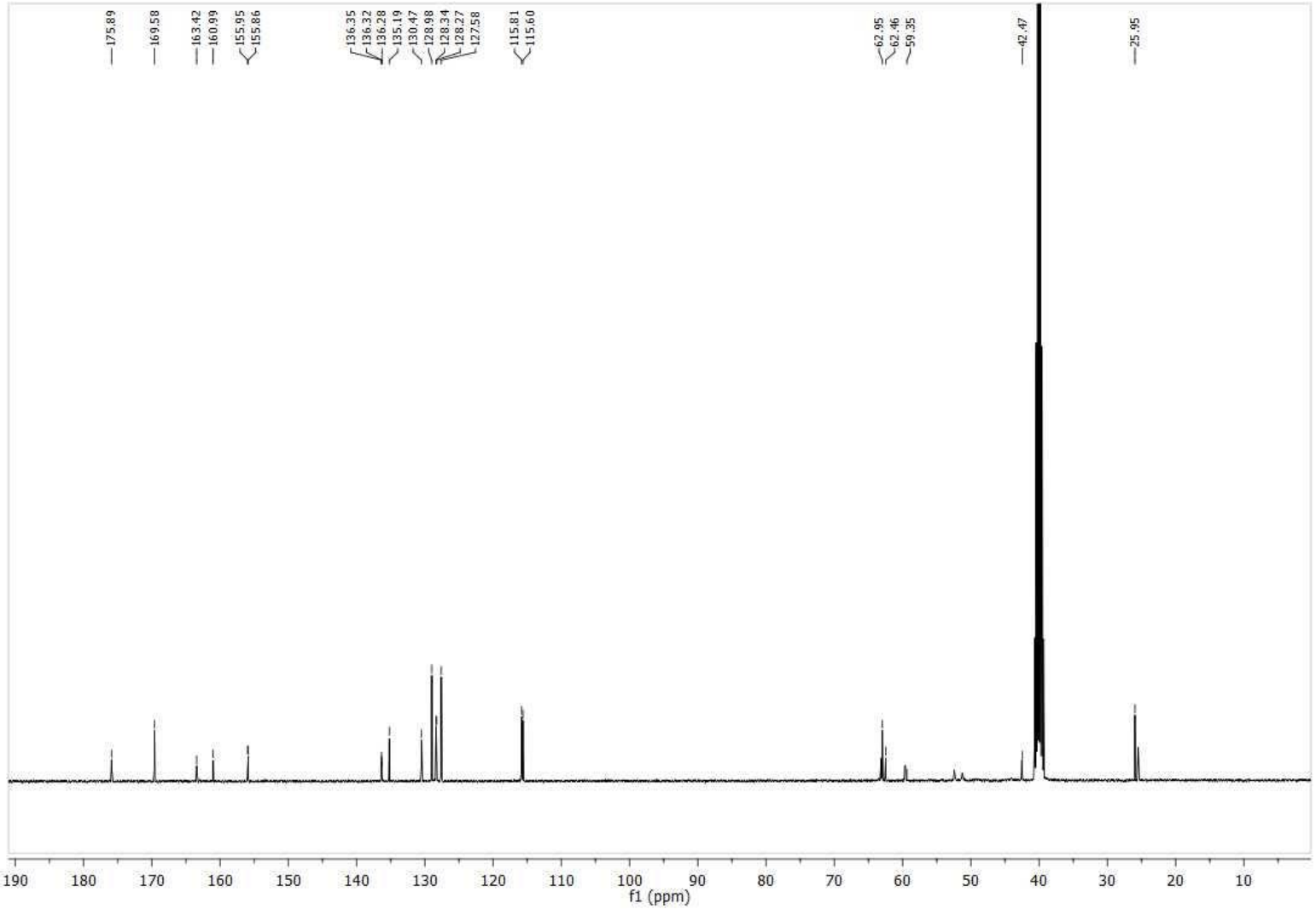

3-[3-(4-benzoylpiperazin-1-yl)-2-hydroxypropyl]-5-(4-fluorophenyl)-5-methylimidazolidine-2,4-dione **(5)**
^{1}H NMR. 300 MHz. DMSO

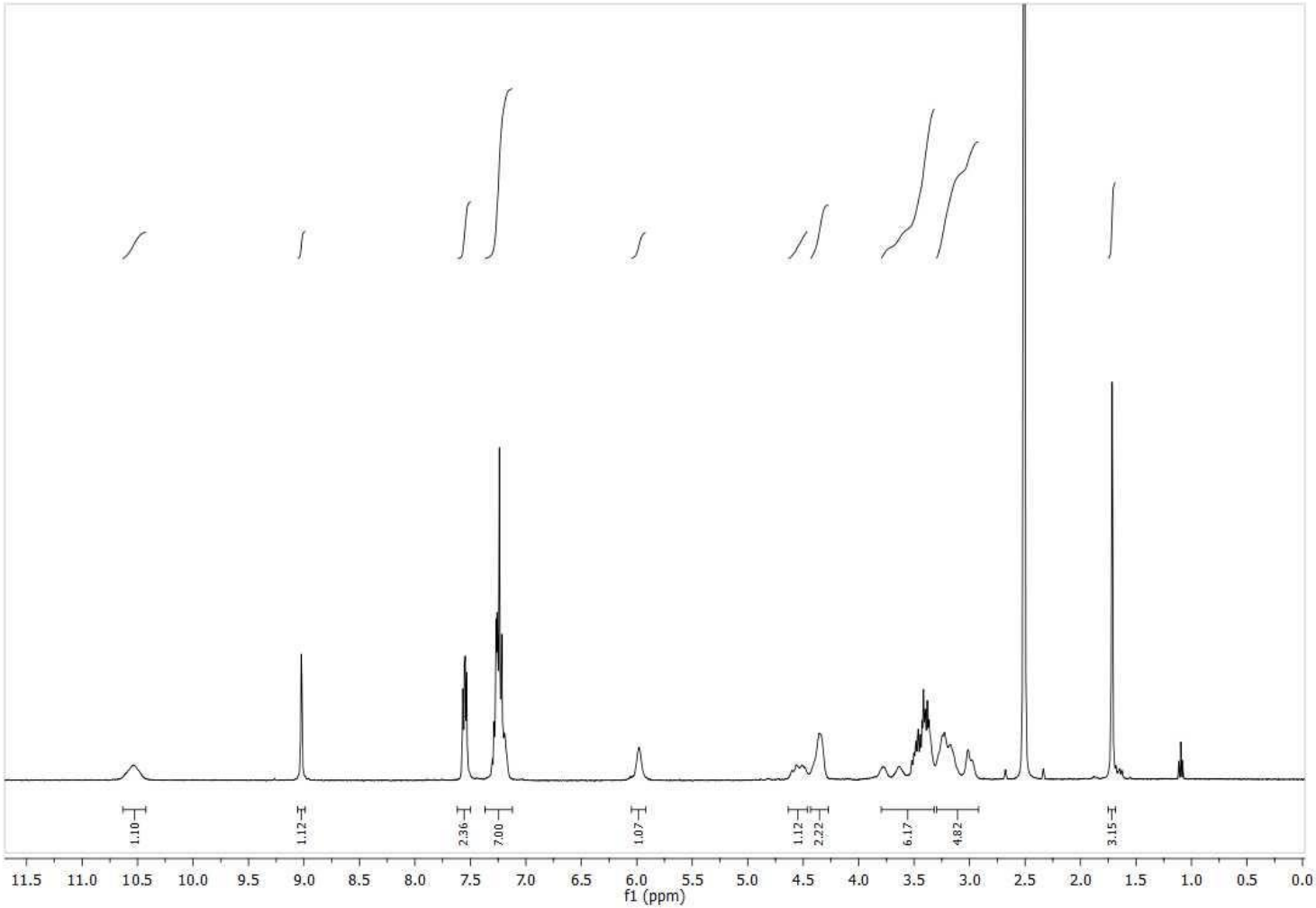

^{13}C NMR. 300 MHz. DMSO

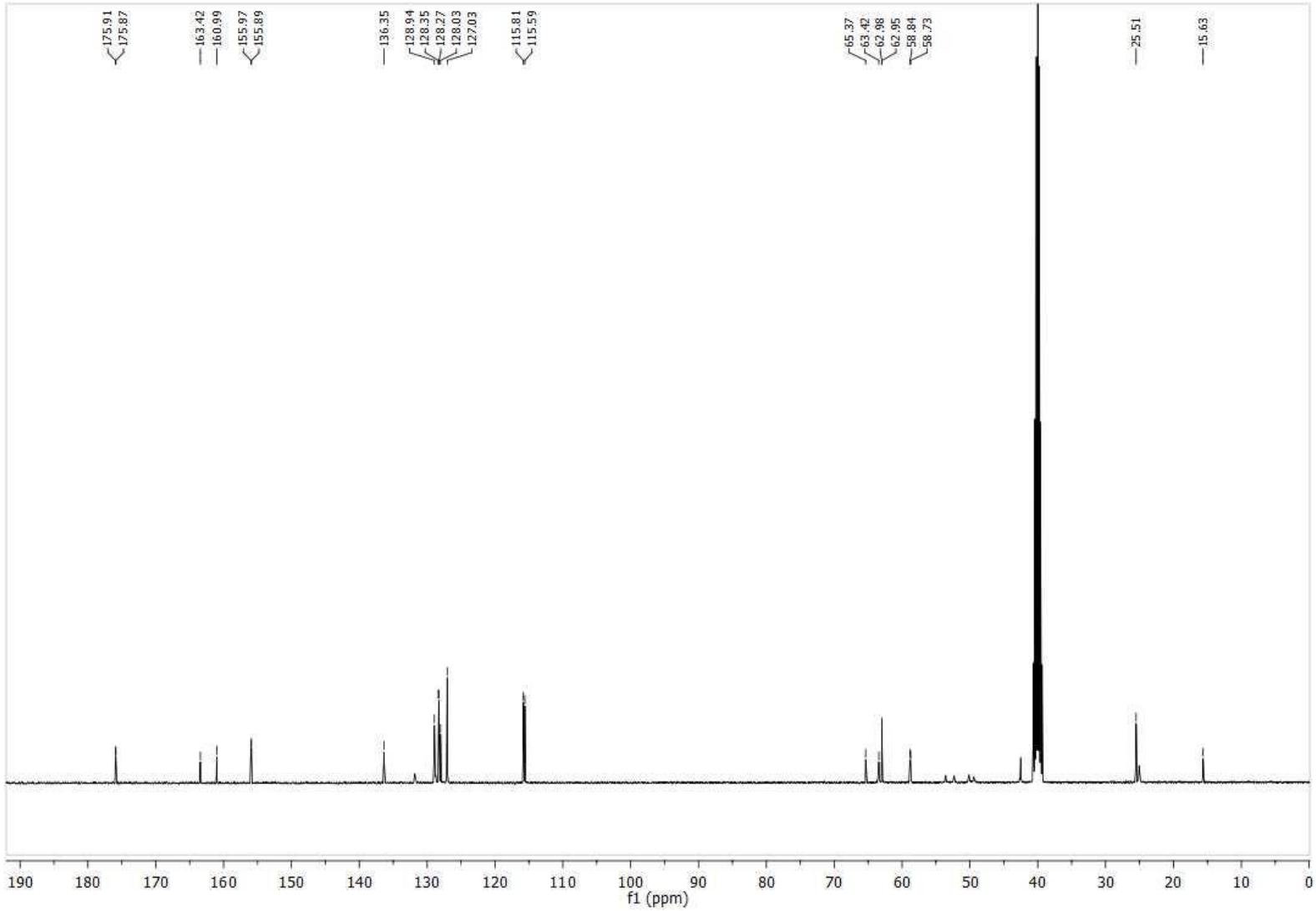

5-(4-fluorophenyl)-3-(2-hydroxy-3-{4-[(naphthalen-1-yl)methyl]piperazin-1-yl}propyl)-5-methylimidazolidine-2,4-dione **(6)**

^{1}H NMR. 300 MHz. DMSO

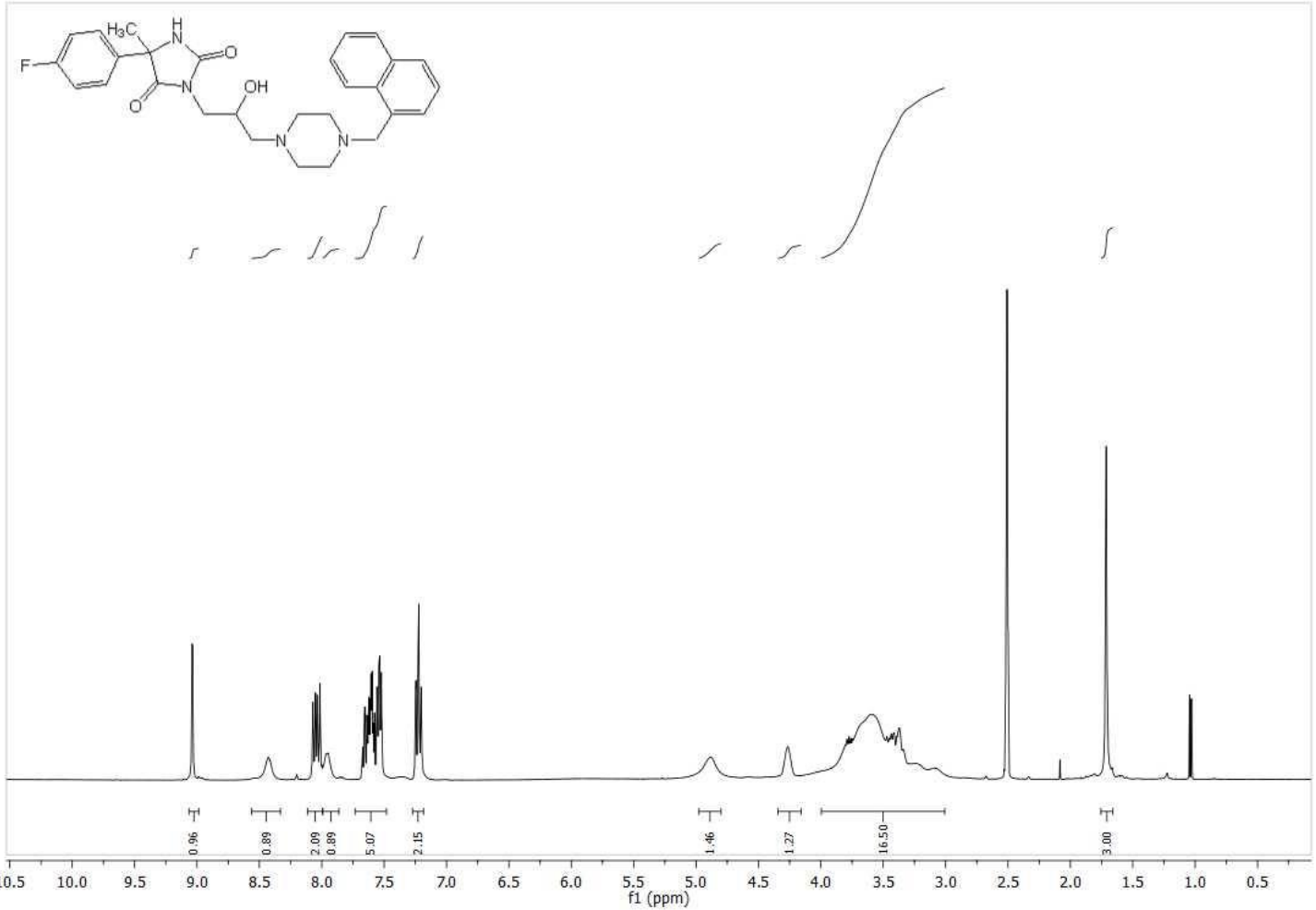

^{13}C NMR. 300 MHz. DMSO

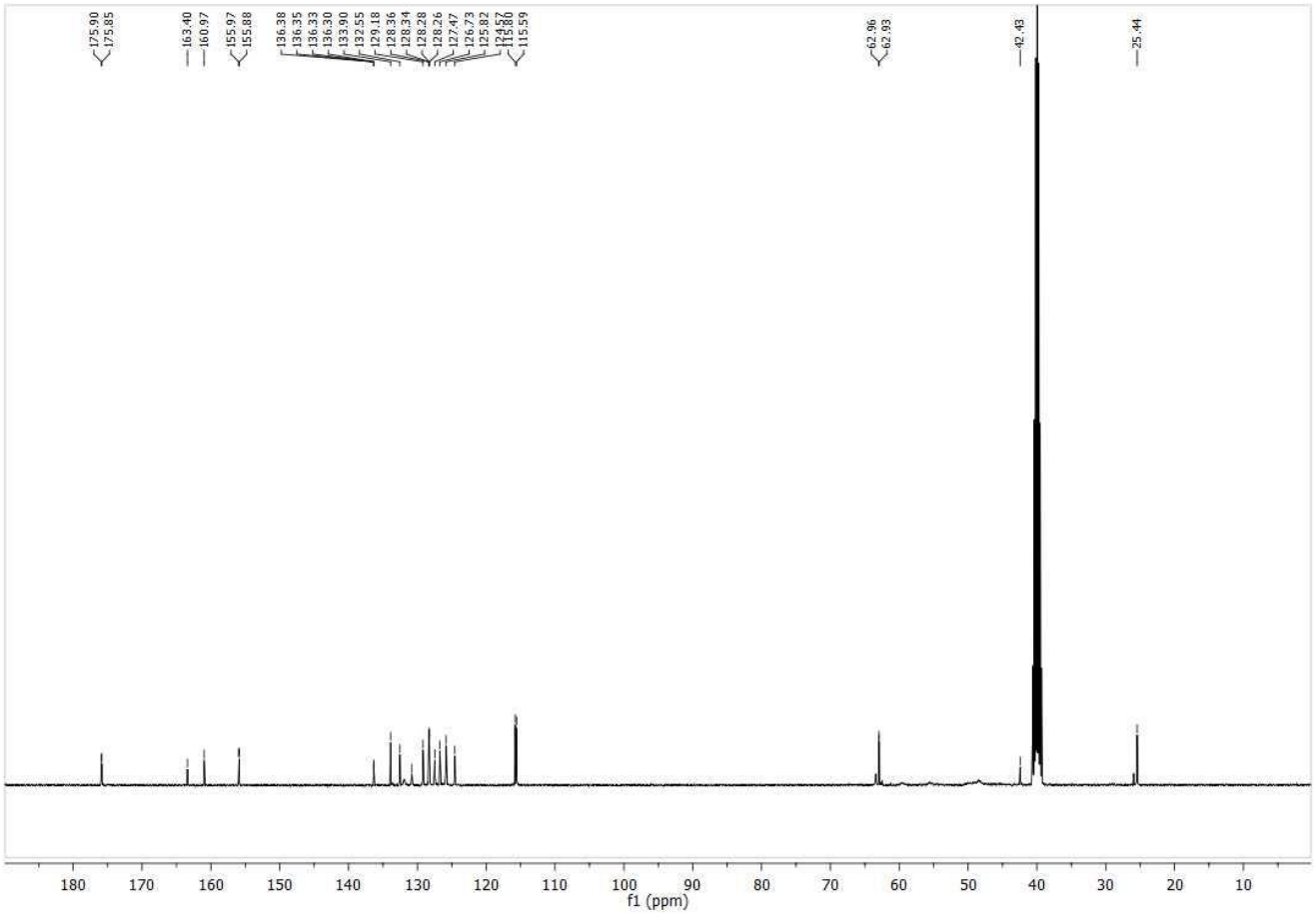

5-(4-fluorophenyl)-3-{2-hydroxy-3-[4-(naphthalen-1-yl)piperazin-1-yl]propyl}-5-methylimidazolidine-2,4-dione **(7)**
^{1}H NMR. 300 MHz. DMSO

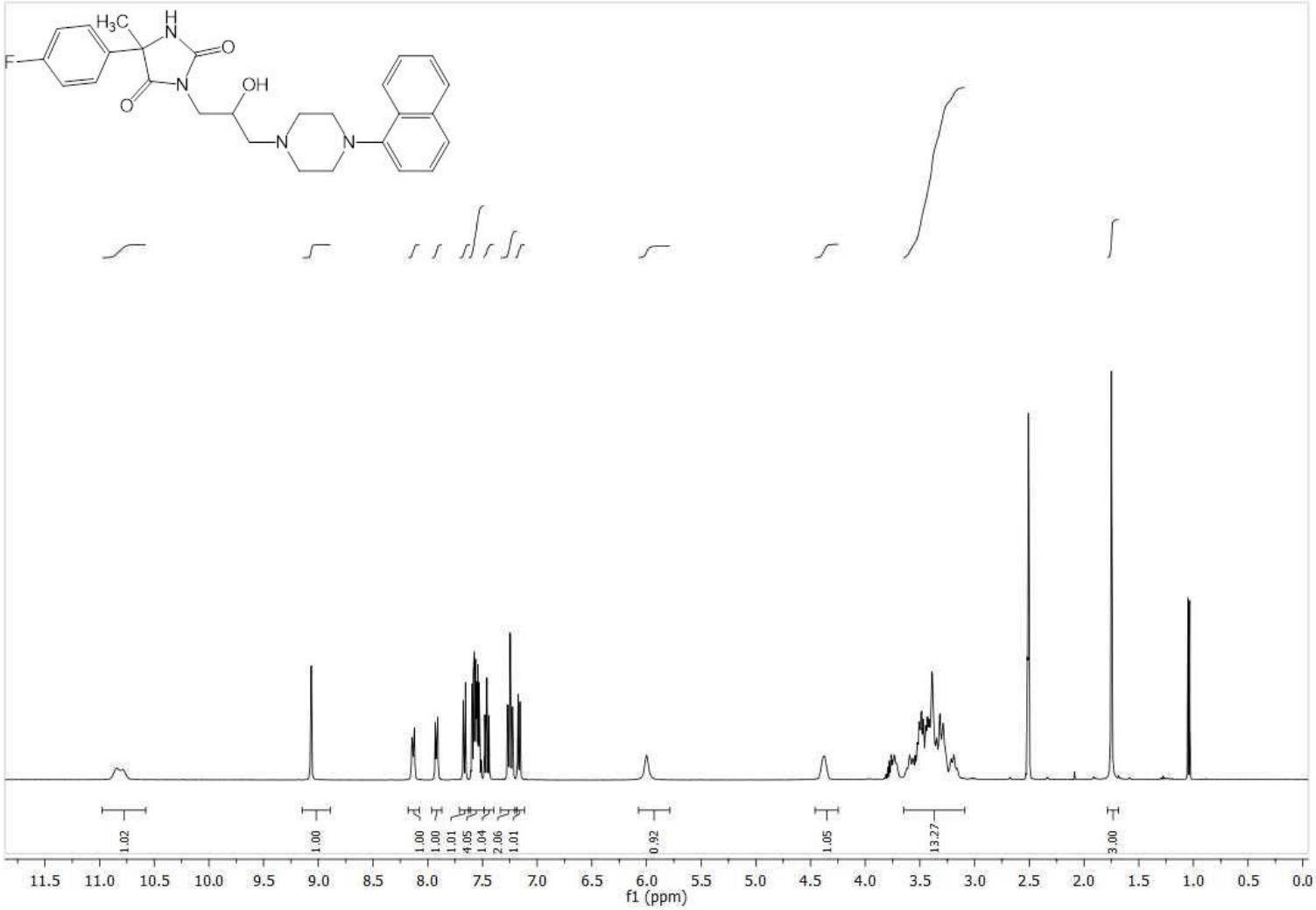

^{13}C NMR. 300 MHz. DMSO

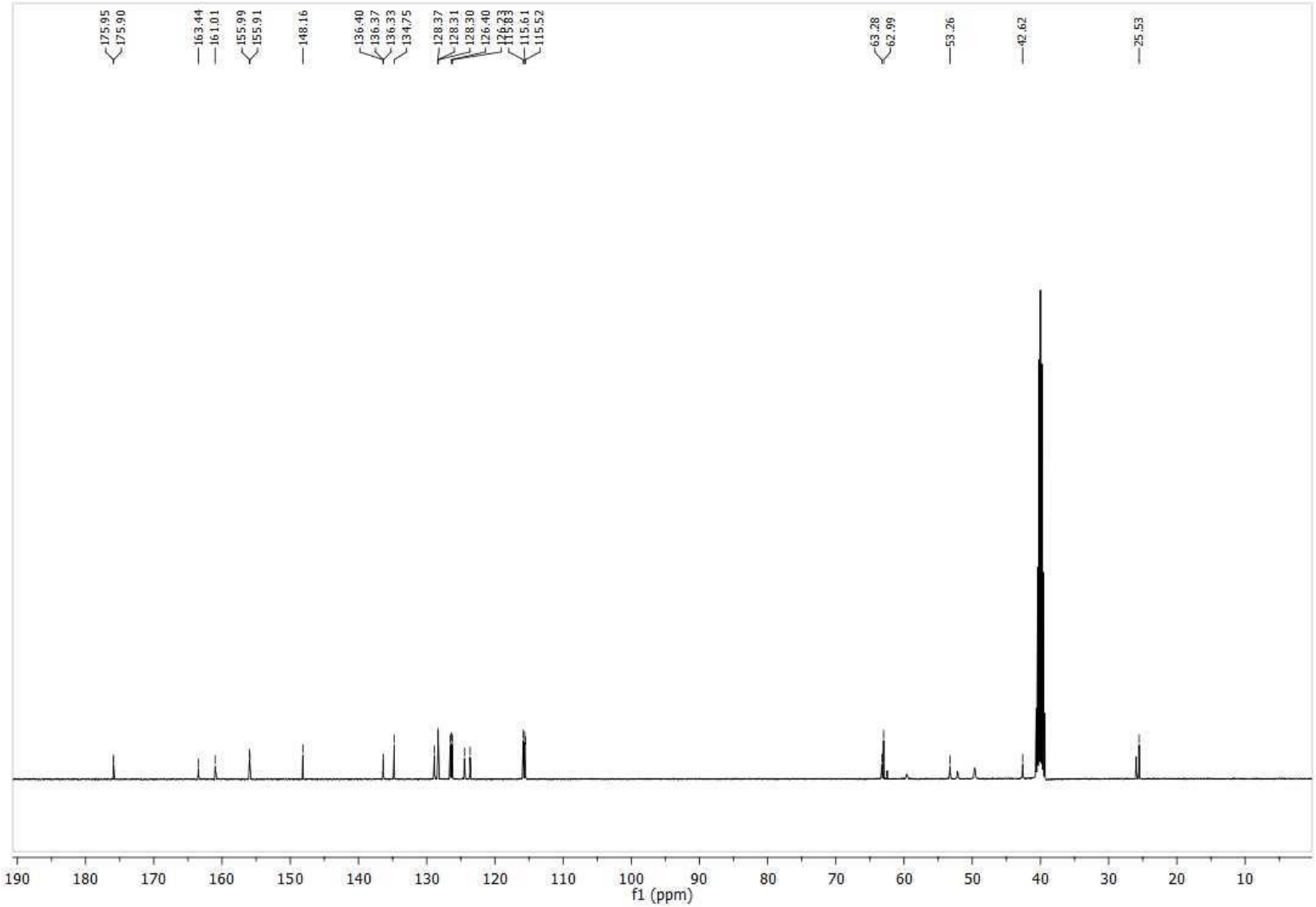

5-(4-fluorophenyl)-3-[2-hydroxy-3-(4-phenoxypiperidin-1-yl)propyl]-5-methylimidazolidine-2,4-dione **(8)**

^{1}H NMR. 300 MHz. DMSO

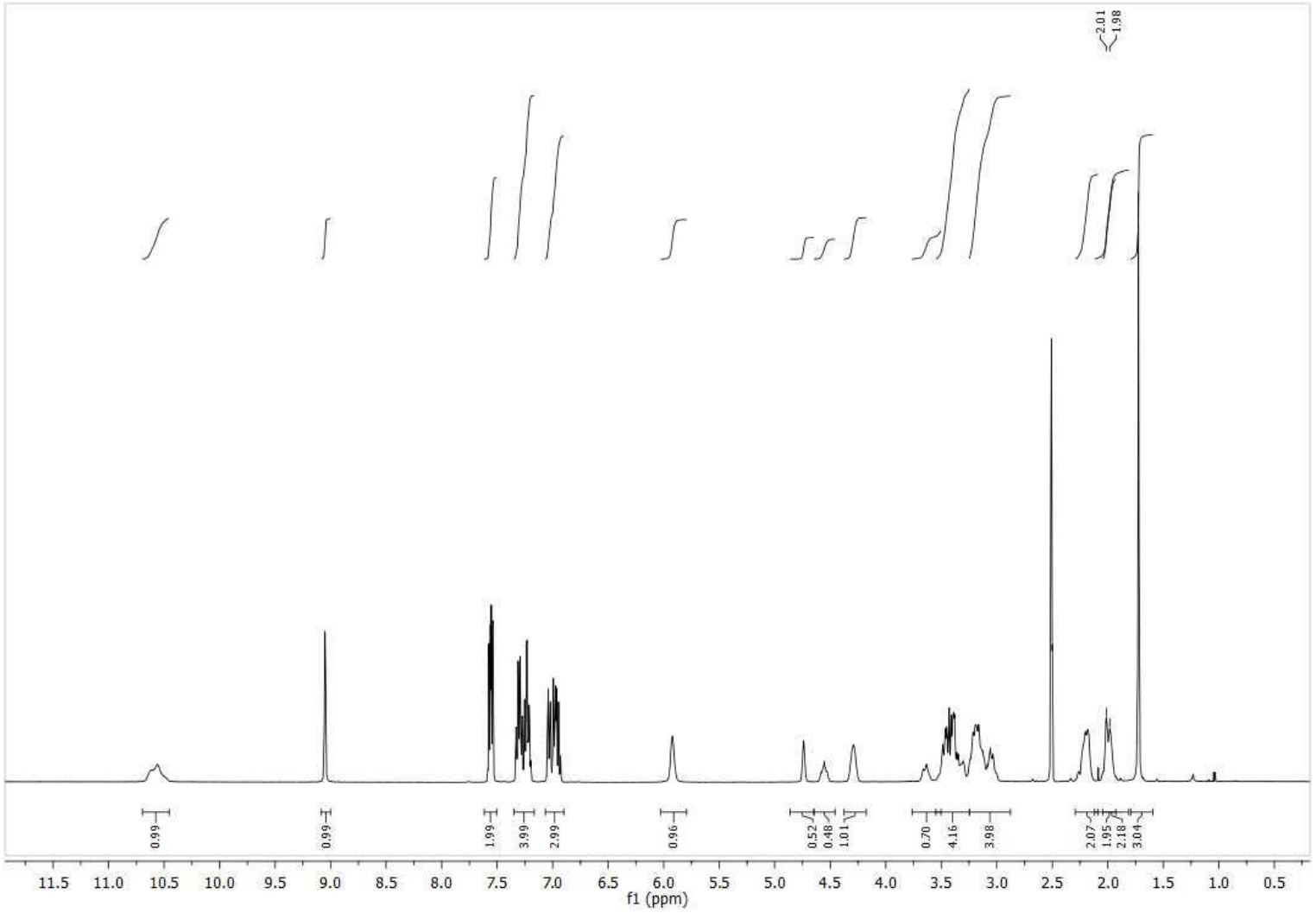

^{13}C NMR. 300 MHz. DMSO

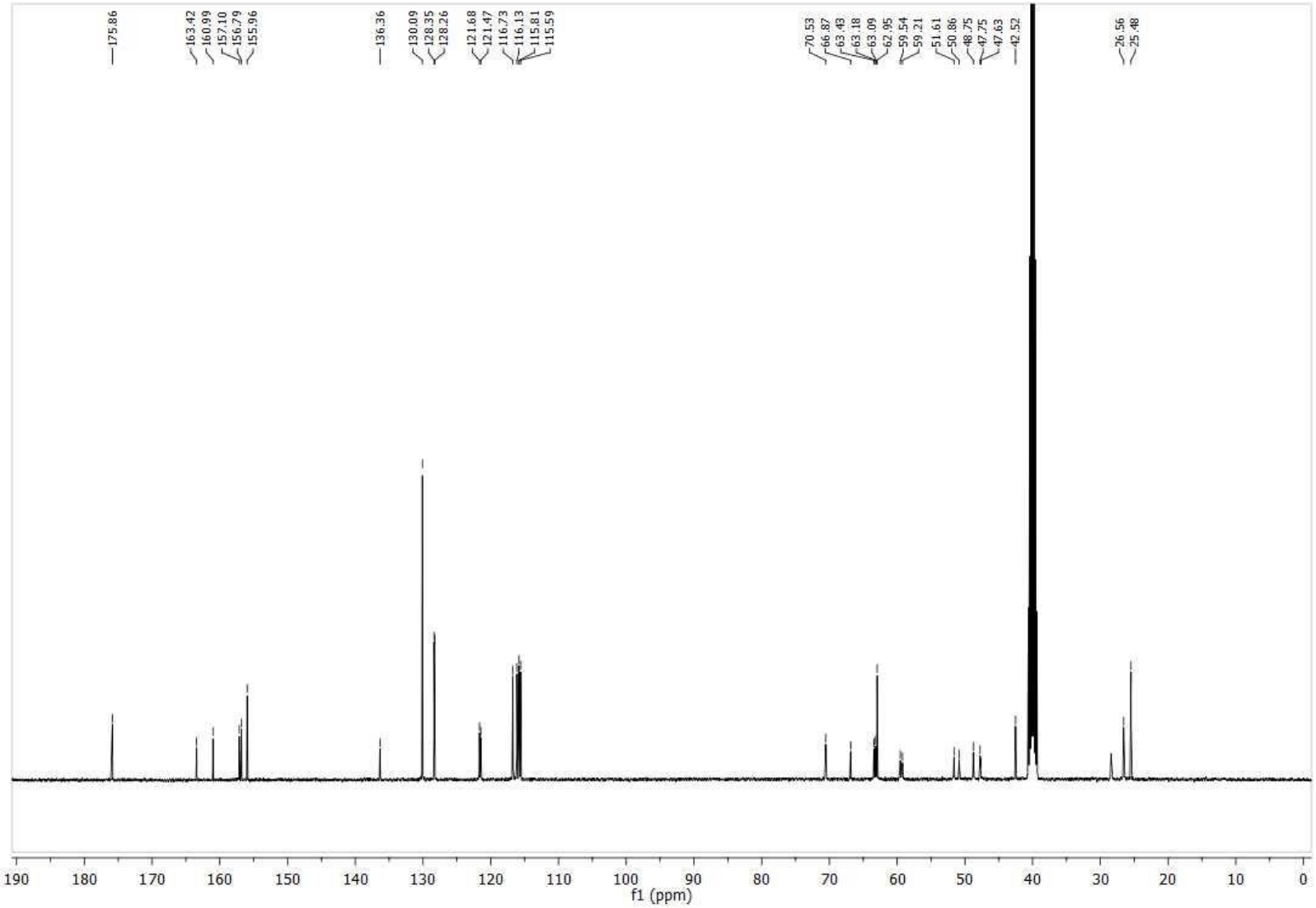

3-{3-[4-(4-chlorophenoxy)piperidin-1-yl]-2-hydroxypropyl}-5-(4-fluorophenyl)-5-methylimidazolidine-2,4-dione **(9)**

^{1}H NMR. 300 MHz. DMSO

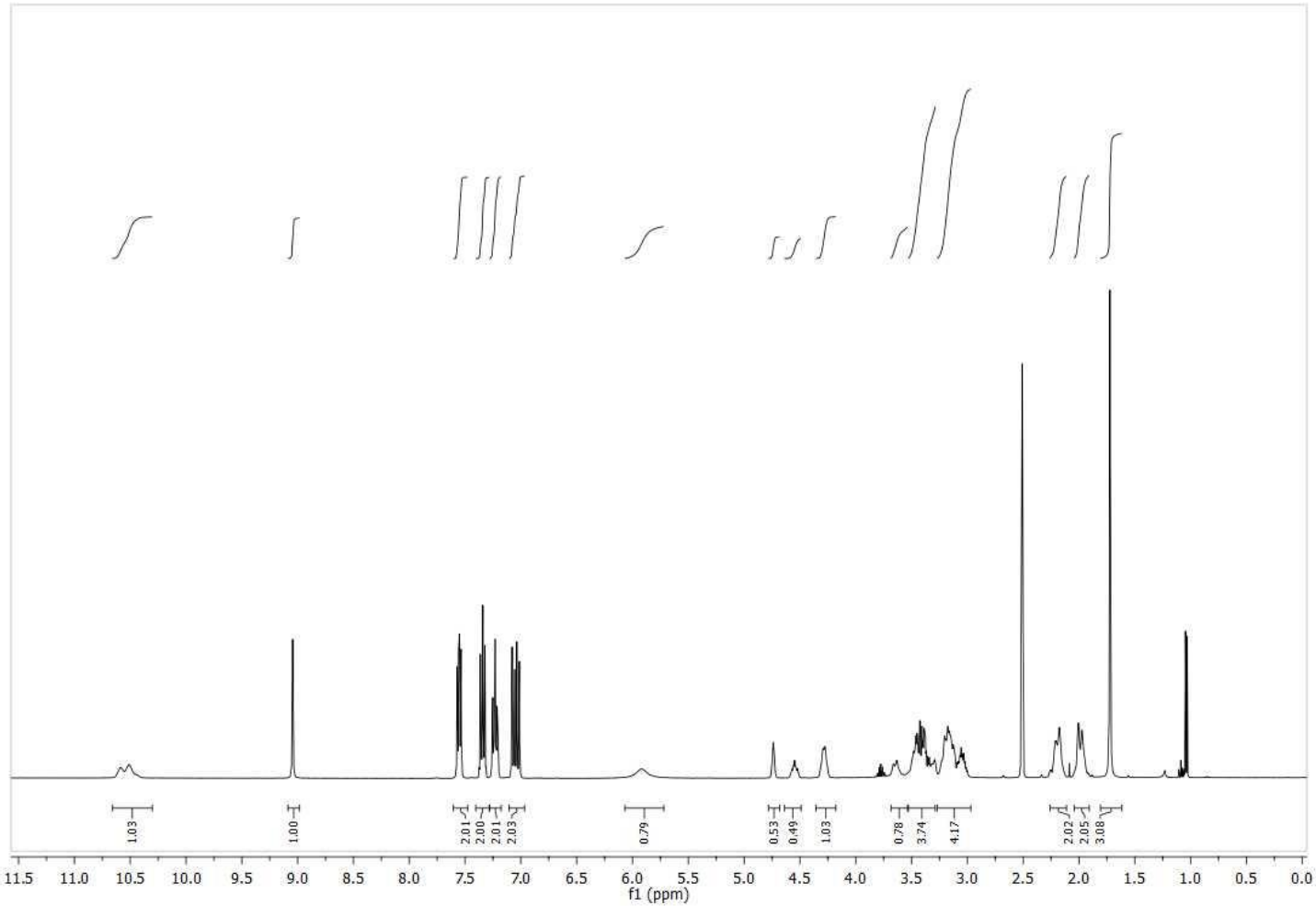

^{13}C NMR. 300 MHz. DMSO

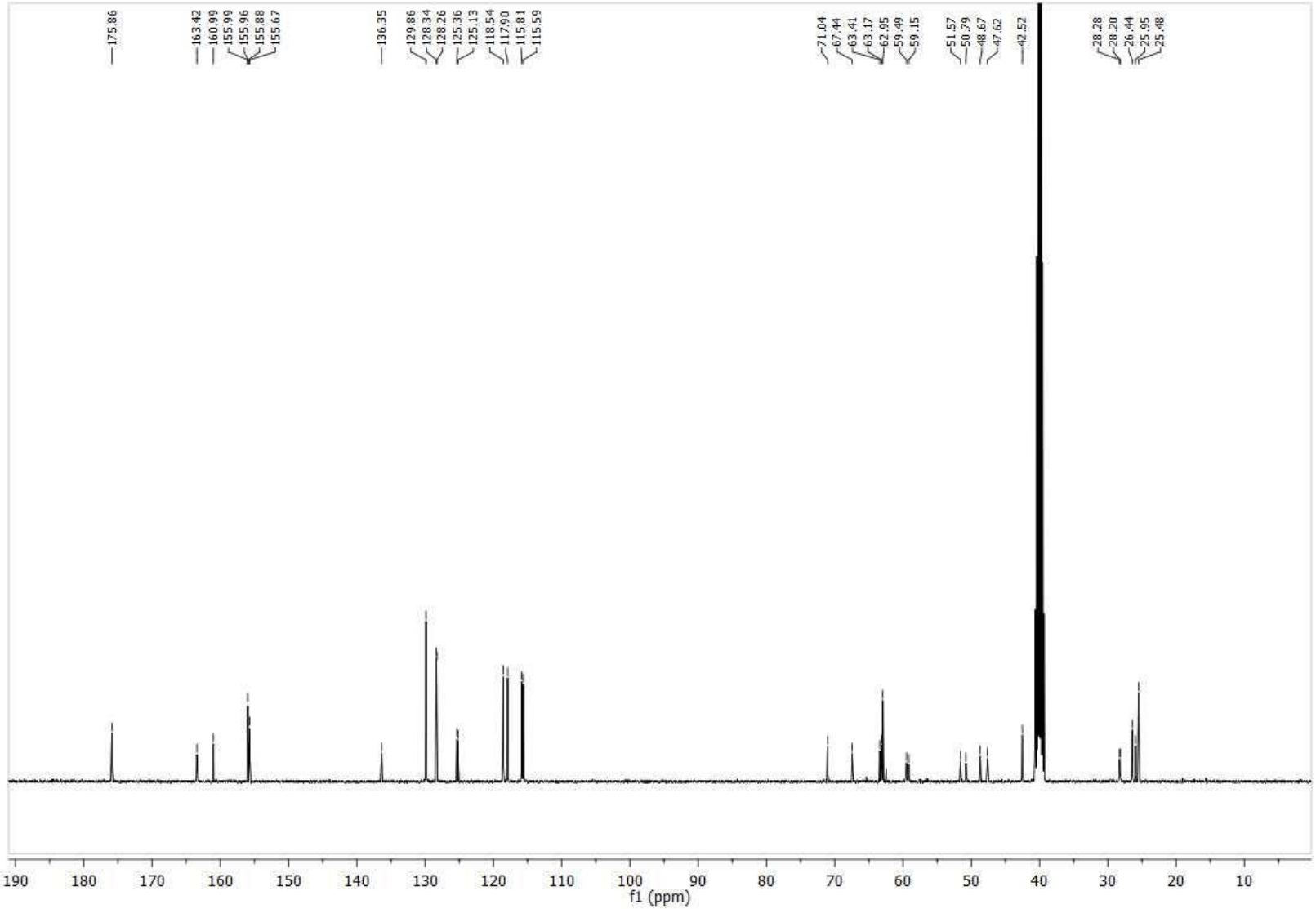

3-{2-hydroxy-3-[4-(2-methoxyphenyl)piperazin-1-yl]propyl}-5-methyl-5-(naphthalen-1-yl)imidazolidine-2,4-dione **(10)**

^{1}H NMR. 300 MHz. DMSO

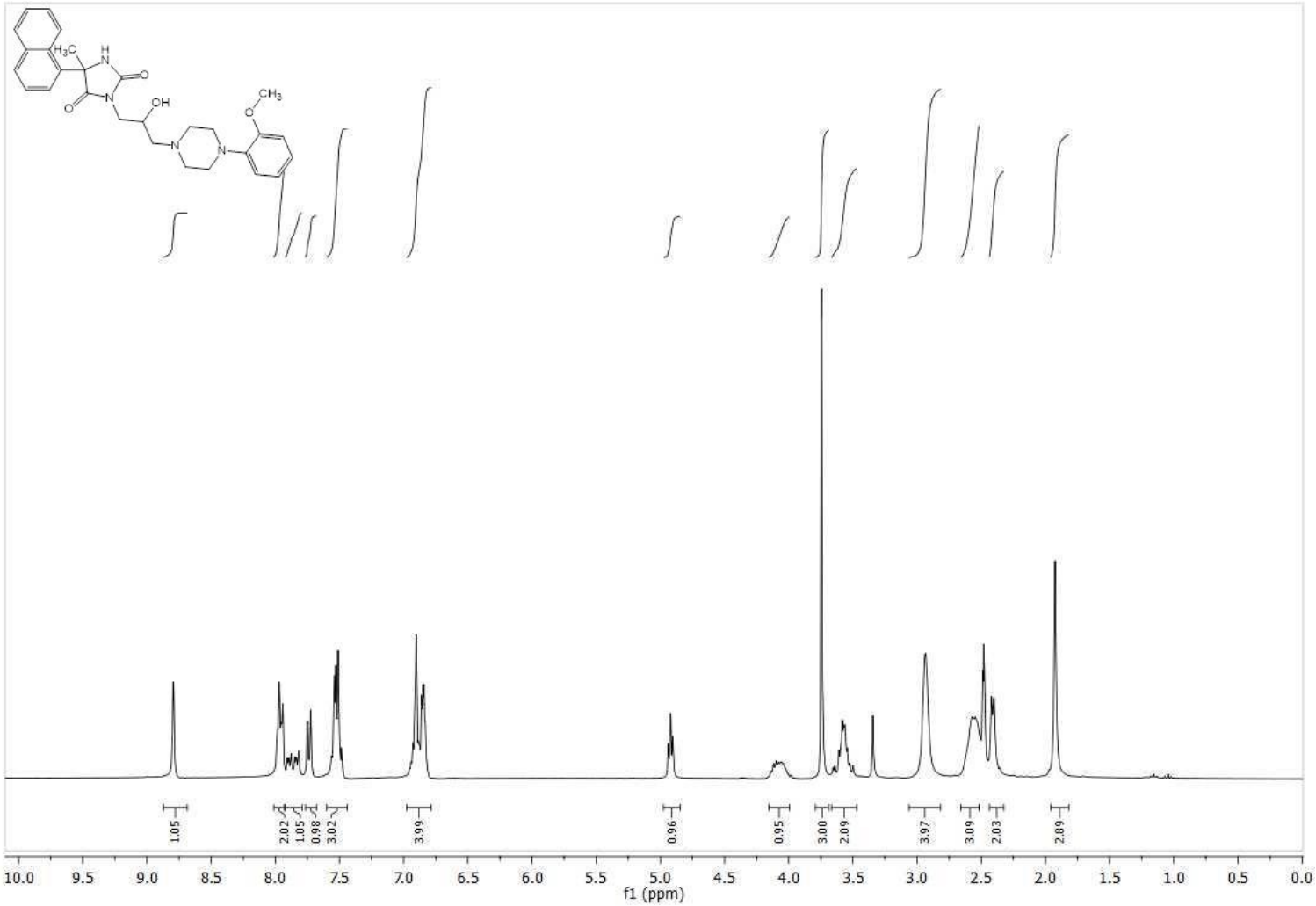

^{13}C NMR. 300 MHz. DMSO

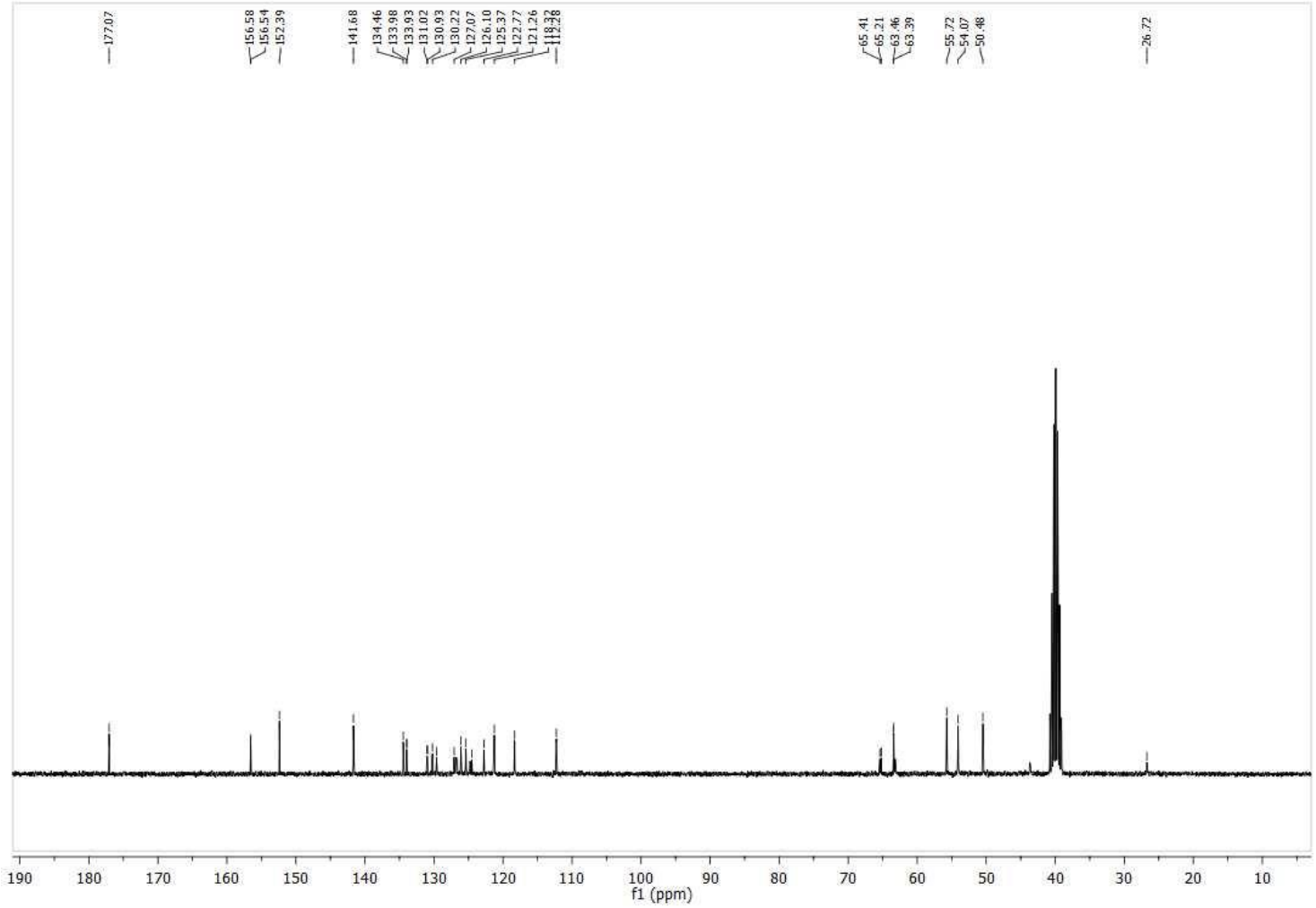

2-(4-{2-hydroxy-3-[4-methyl-4-(naphthalen-1-yl)-2,5-dioxoimidazolidin-1-yl]propyl}piperazin-1-yl)benzonitrile hydrochloride **(11)**

^{1}H NMR. 300 MHz. DMSO

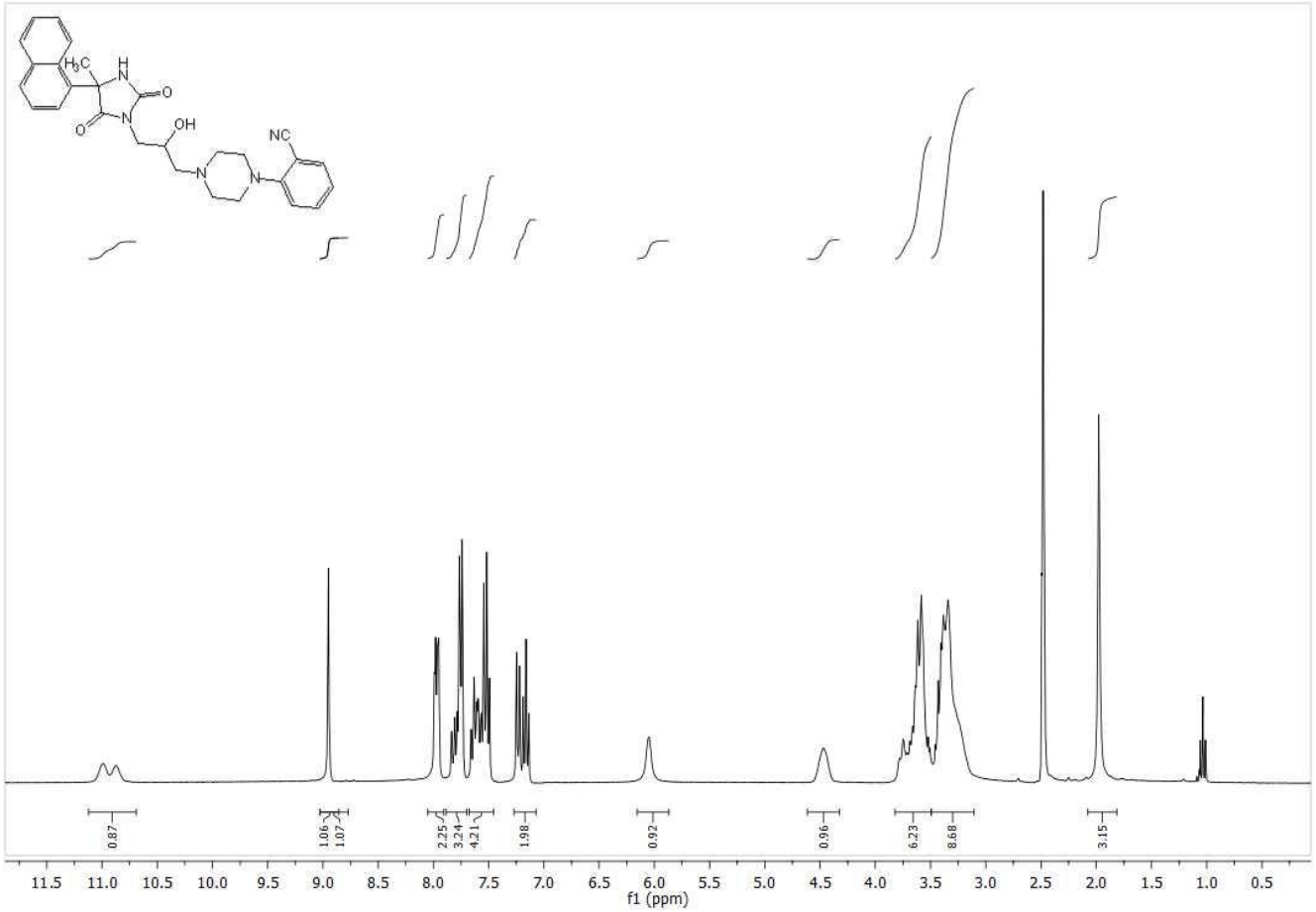

^{13}C NMR. 300 MHz. DMSO

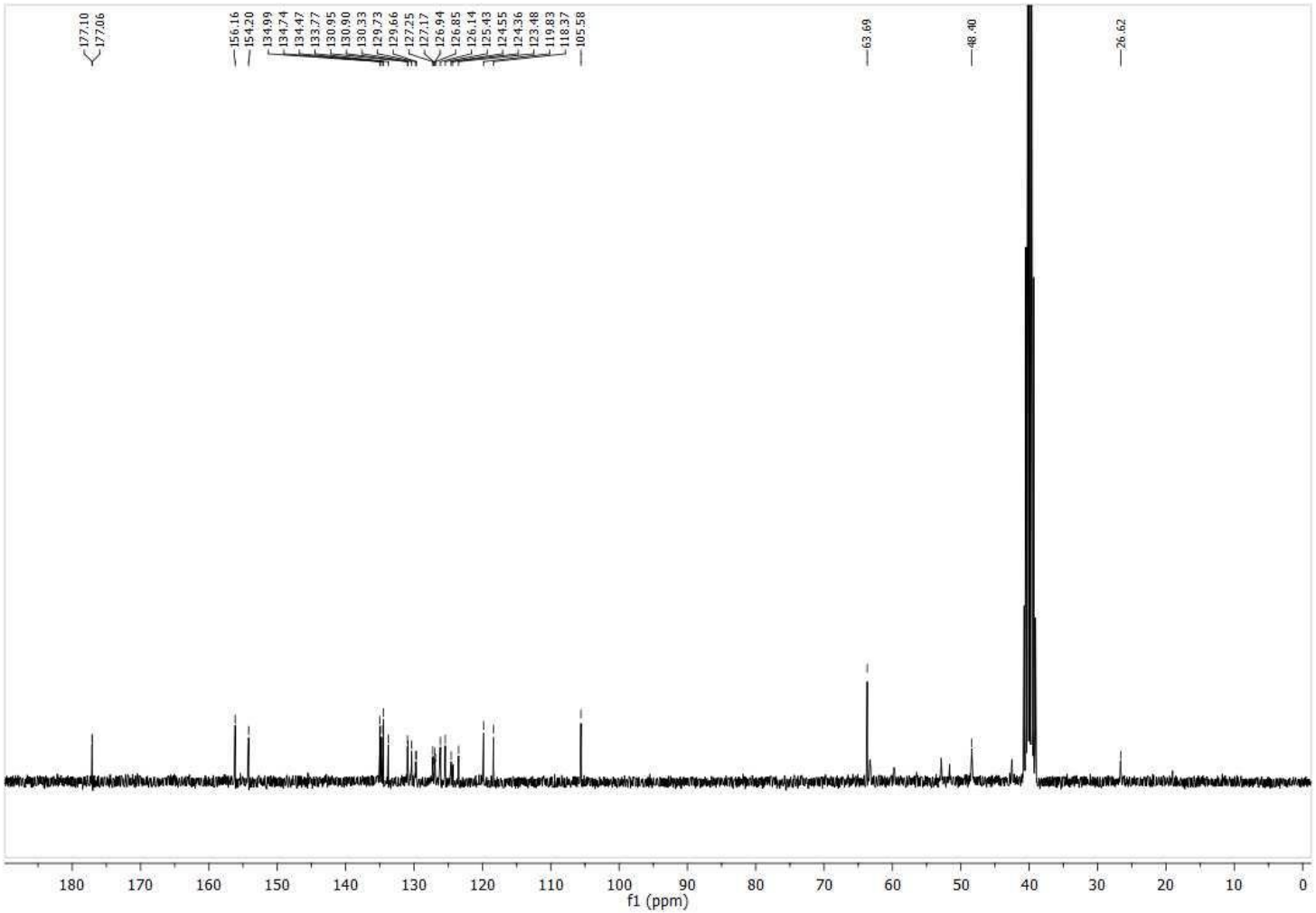

3-{3-[4-(diphenylmethyl)piperazin-1-yl]-2-hydroxypropyl}-5-methyl-5-(naphthalen-1-yl)imidazolidine-2,4-dione **(12)**

^{1}H NMR. 300 MHz. DMSO

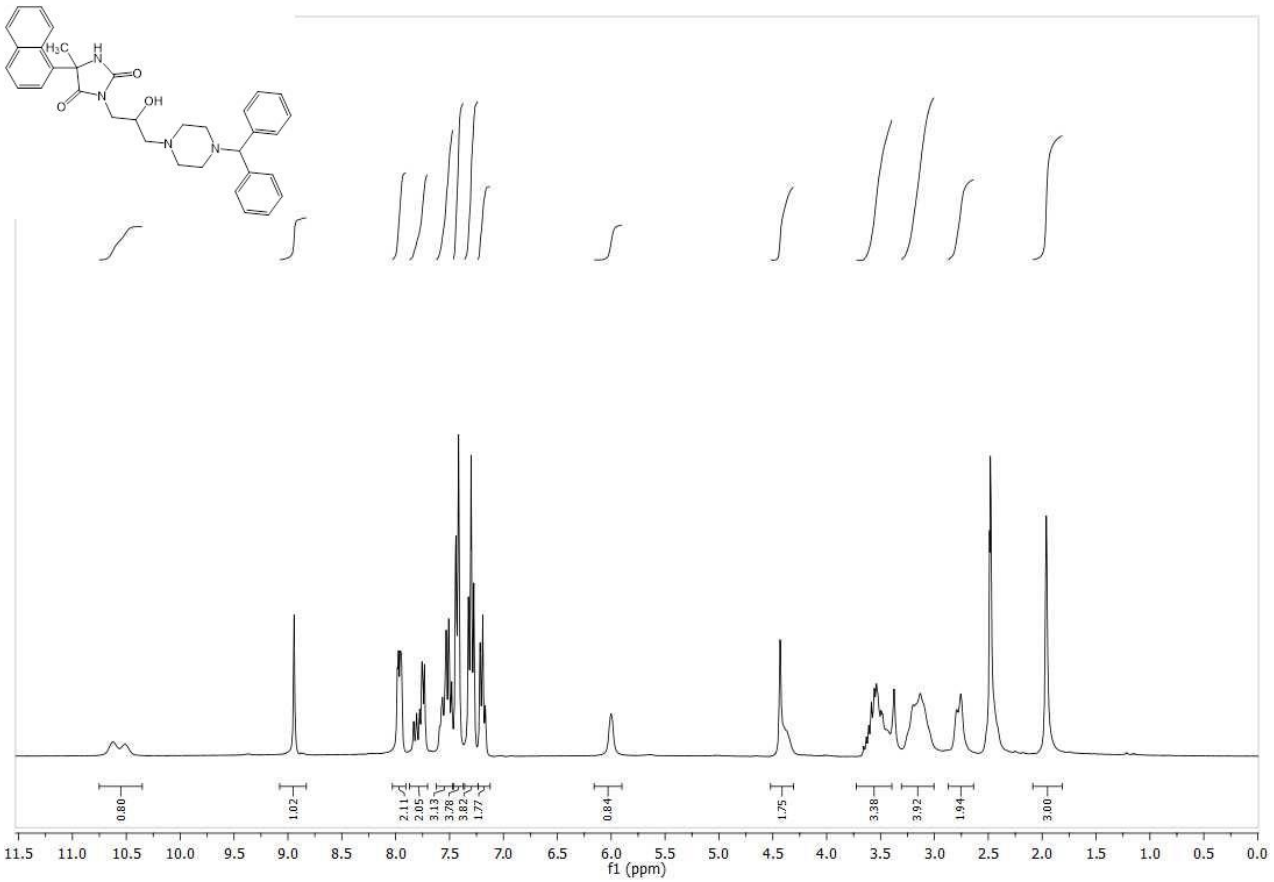

^{13}C NMR. 300 MHz. DMSO

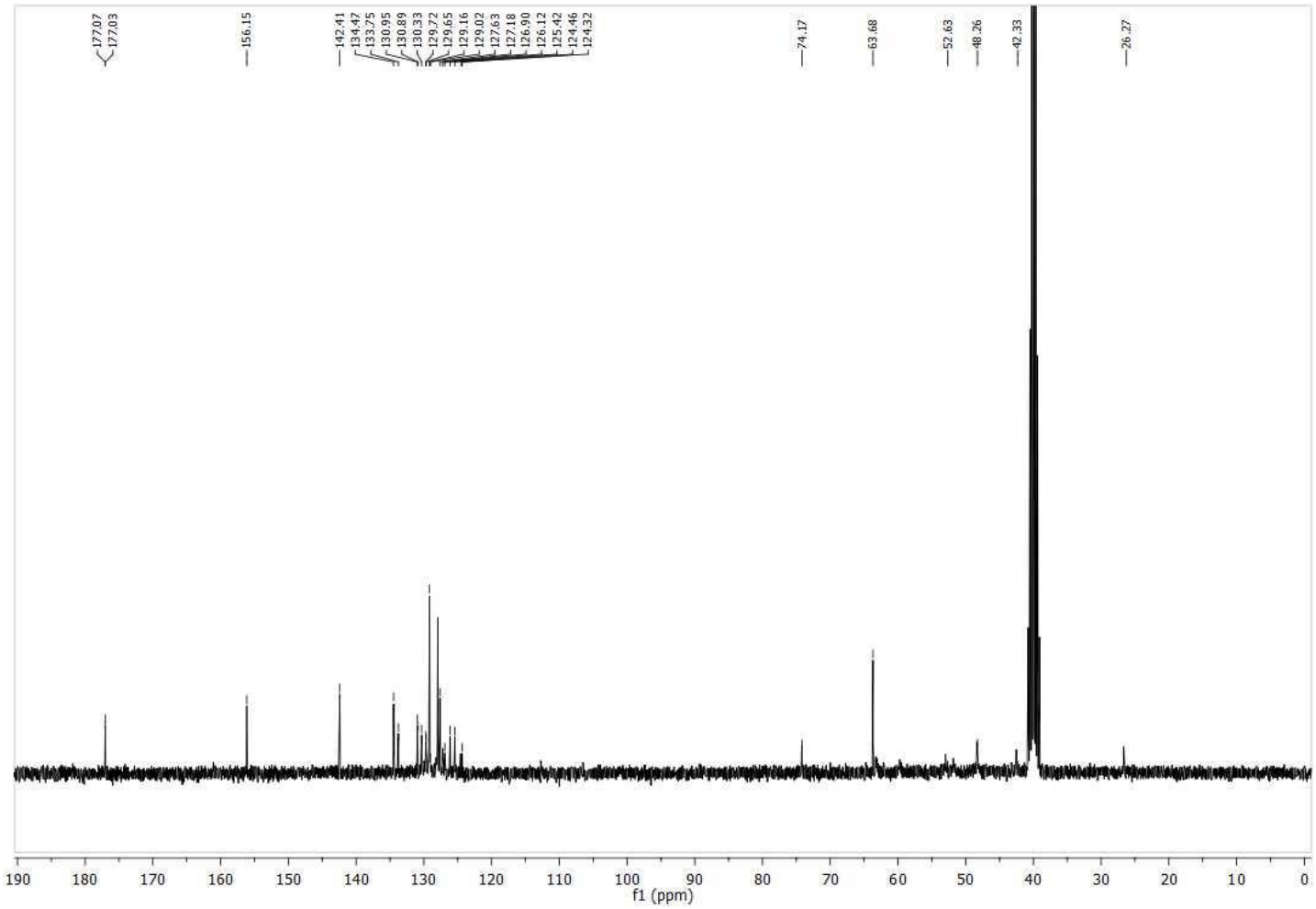

3-{2-hydroxy-3-[4-(2-methoxyphenyl)piperazin-1-yl]propyl}-5-methyl-5-(naphthalen-2-yl)imidazolidine-2,4-dione hydrochloride **(13)**

^{1}H NMR. 300 MHz. DMSO

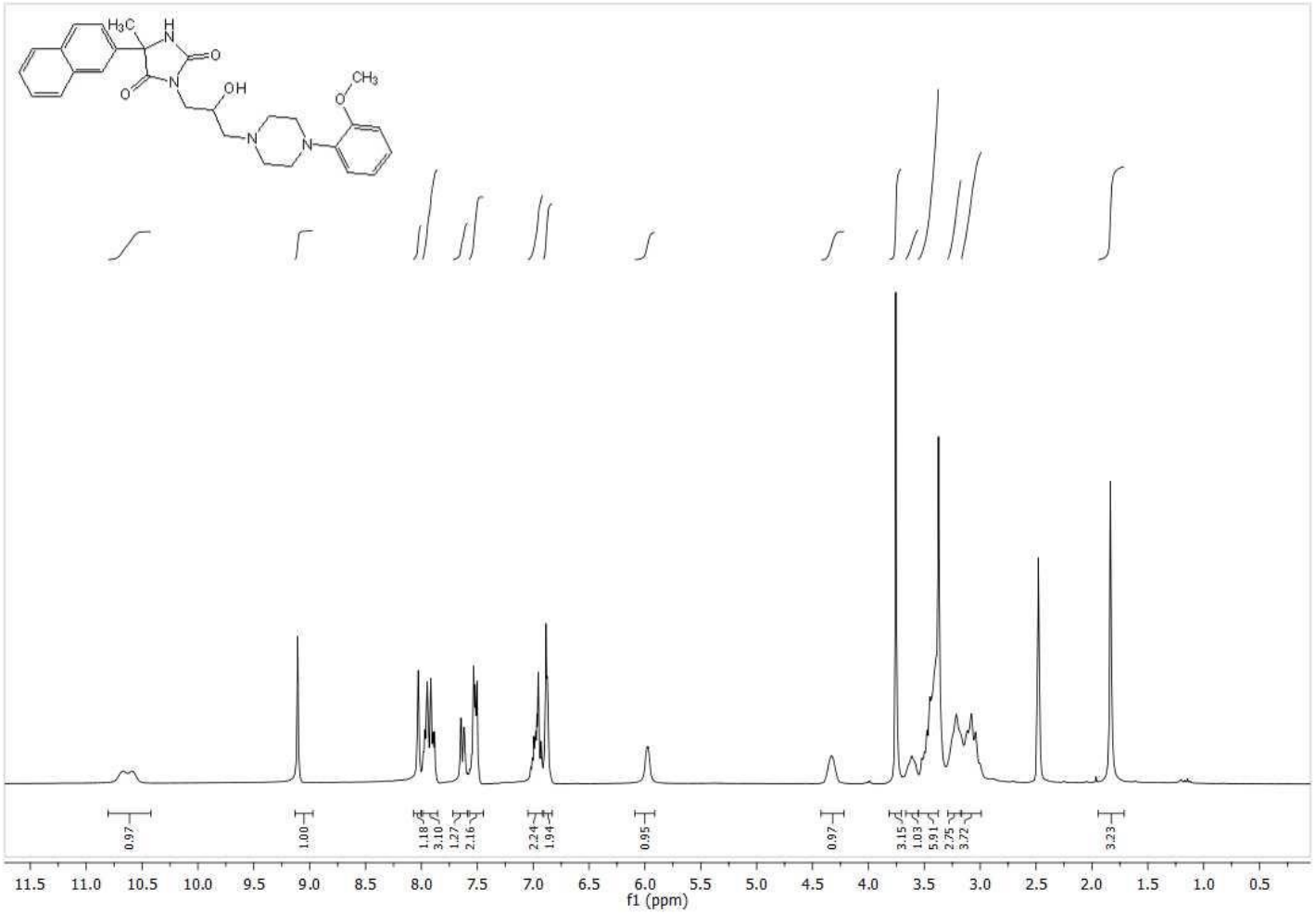

^{13}C NMR. 300 MHz. DMSO

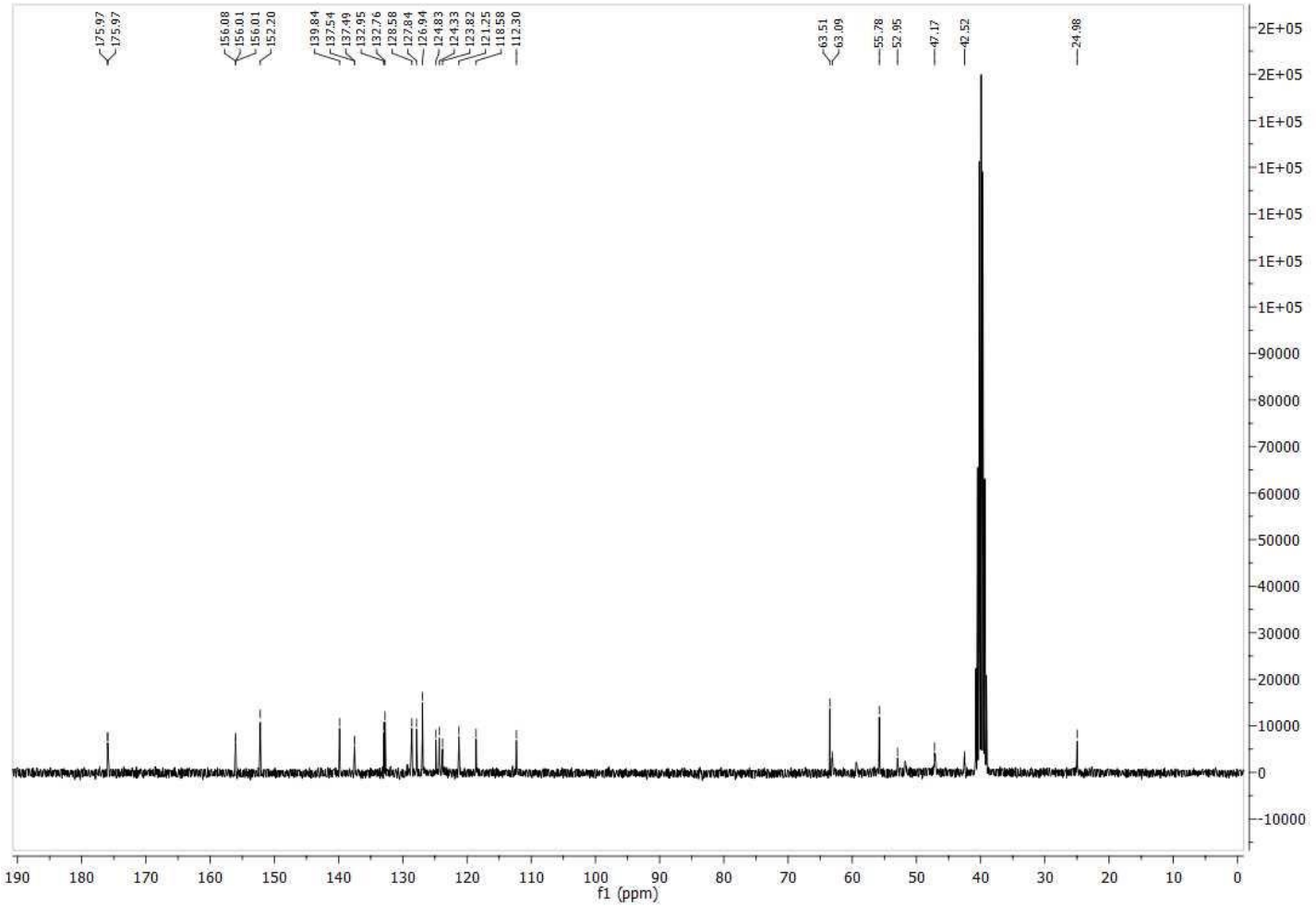

2-(4-{2-hydroxy-3-[4-methyl-4-(naphthalen-2-yl)-2,5-dioxoimidazolidin-1-yl]propyl}piperazin-1-yl)benzonitrile **(14)**

^{1}H NMR. 300 MHz. DMSO

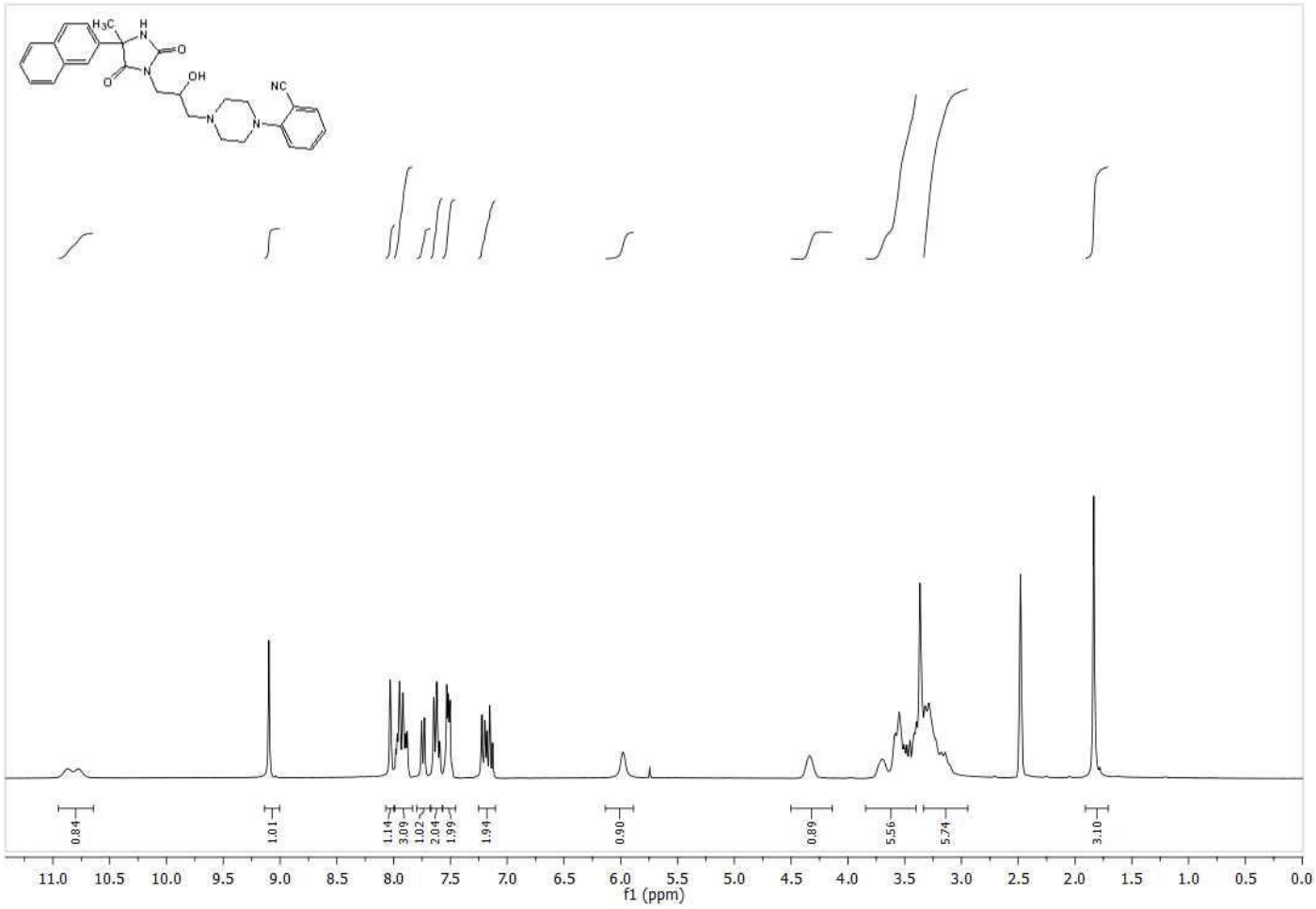

^{13}C NMR. 300 MHz. DMSO

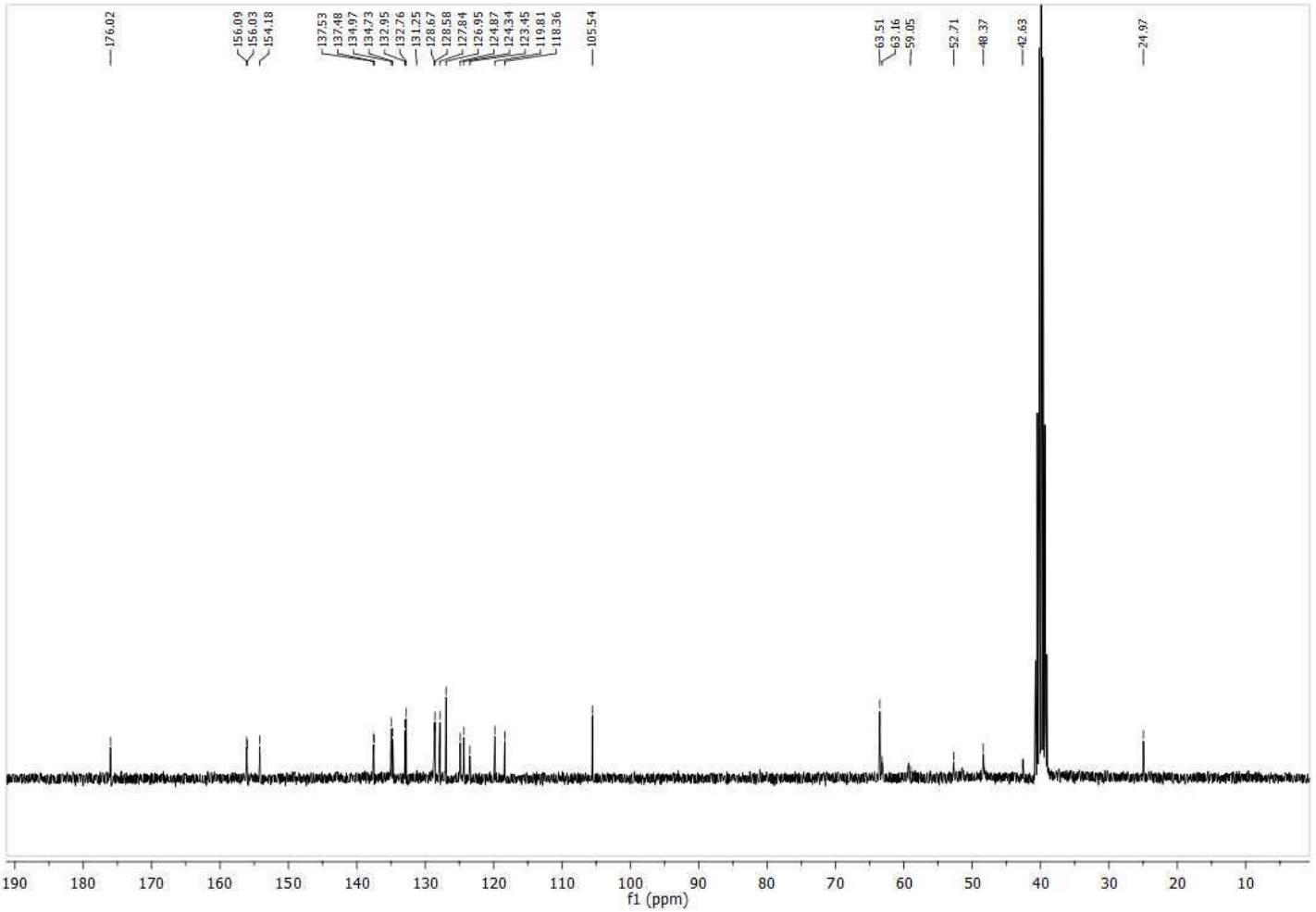

3-{2-hydroxy-3-[4-(2-methoxyphenyl)piperazin-1-yl]propyl}-5,5-dimethylimidazolidine-2,4-dione **(15)**

^{1}H NMR. 300 MHz. DMSO

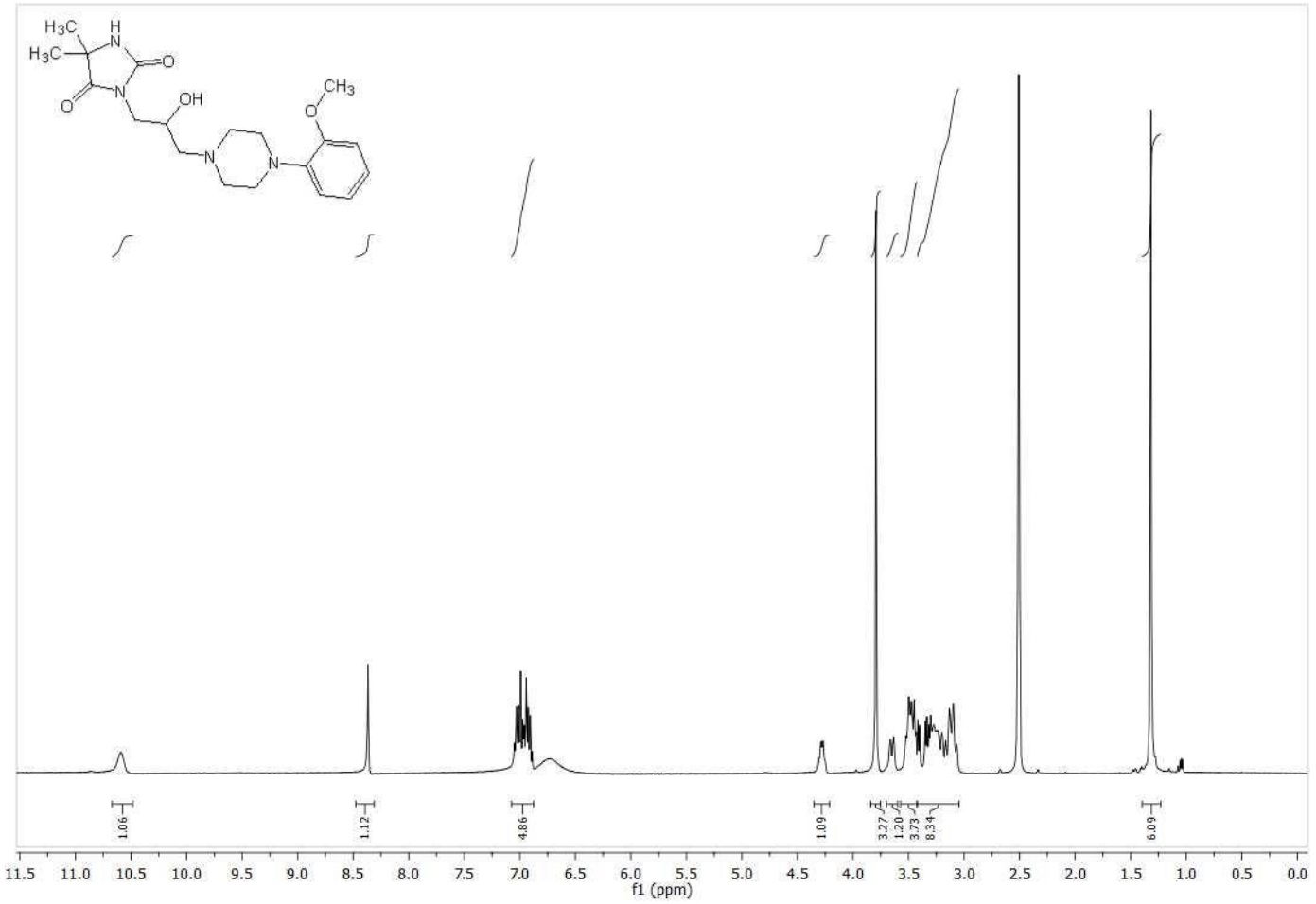

1

^{13}C NMR. 300 MHz. DMSO

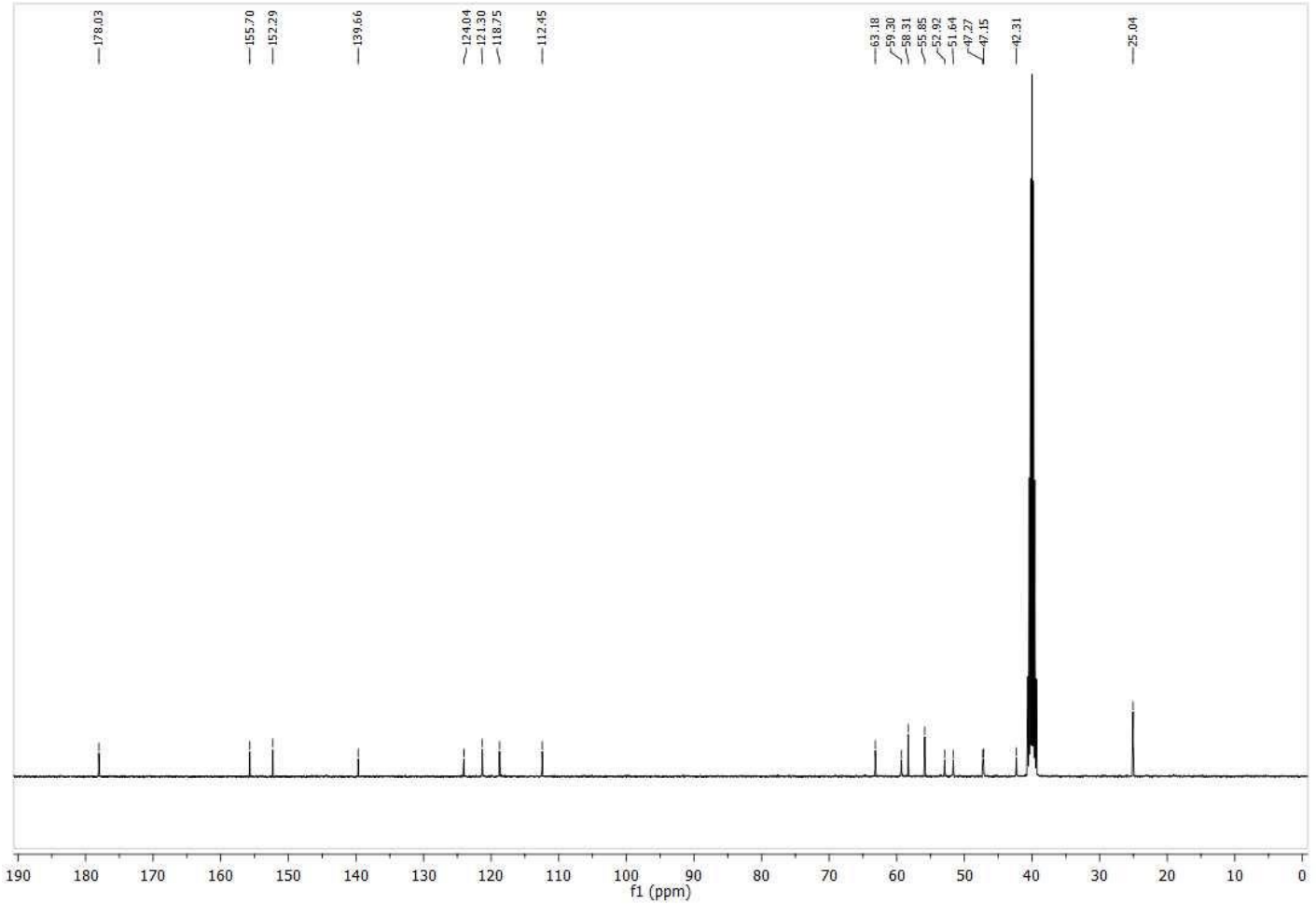

2-{4-[3-(4,4-dimethyl-2,5-dioxoimidazolidin-1-yl)-2-hydroxypropyl]piperazin-1-yl}benzonitrile **(16)**

^{1}H NMR. 300 MHz. DMSO

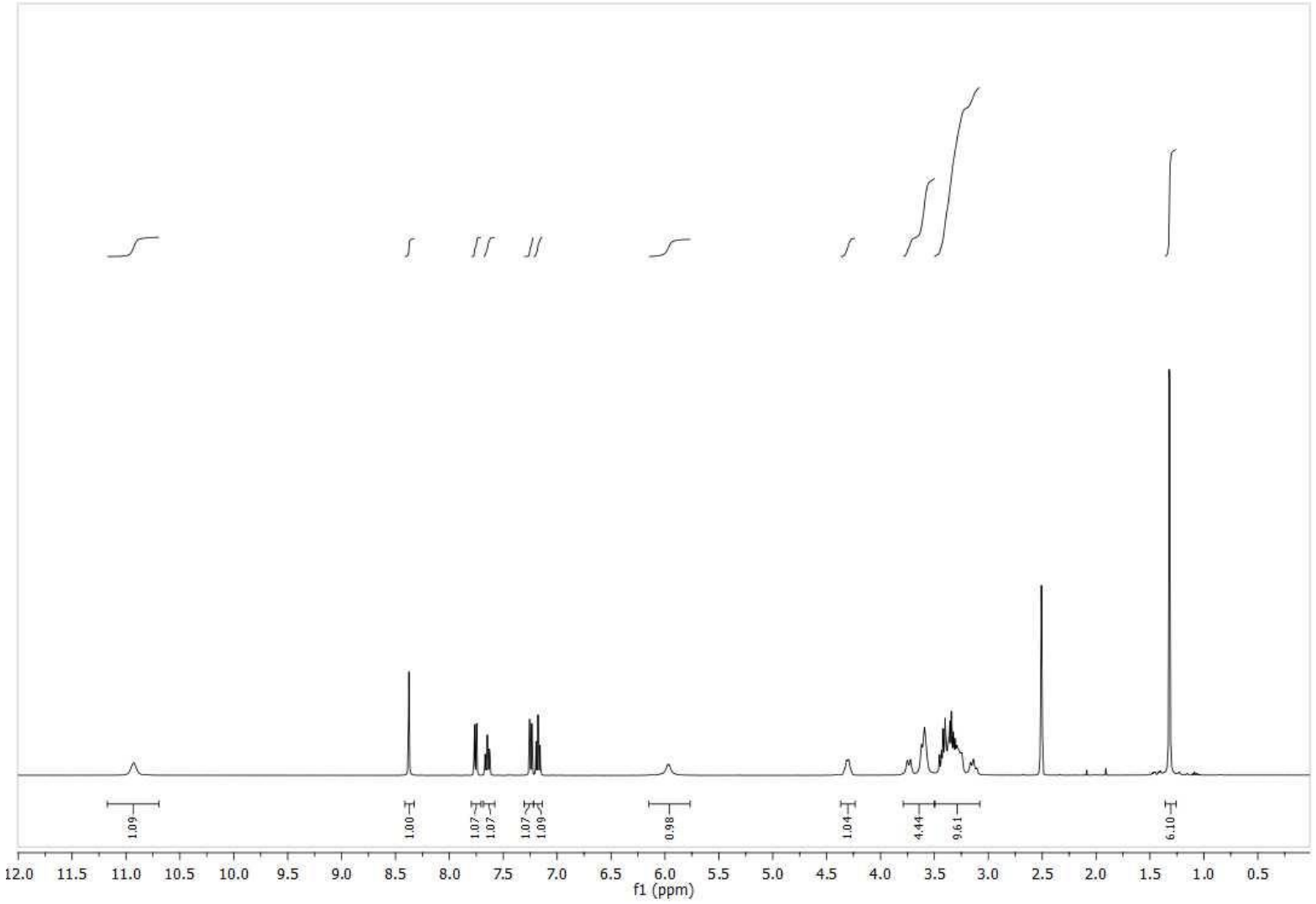

^{13}C NMR. 300 MHz. DMSO

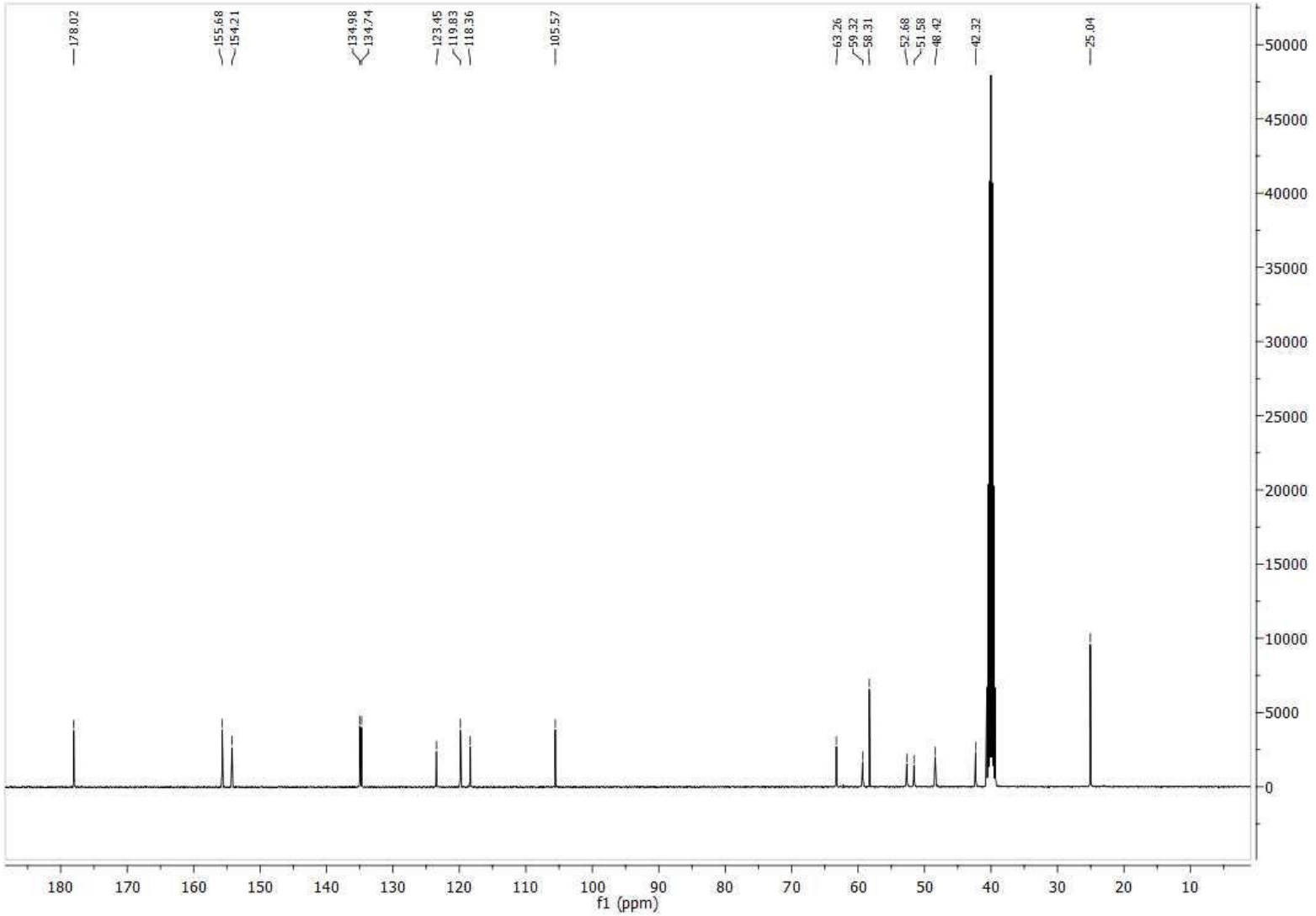

3-{3-[4-(diphenylmethyl)piperazin-1-yl]-2-hydroxypropyl}-5,5-dimethylimidazolidine-2,4-dione **(17)**

^{1}H NMR. 300 MHz. DMSO

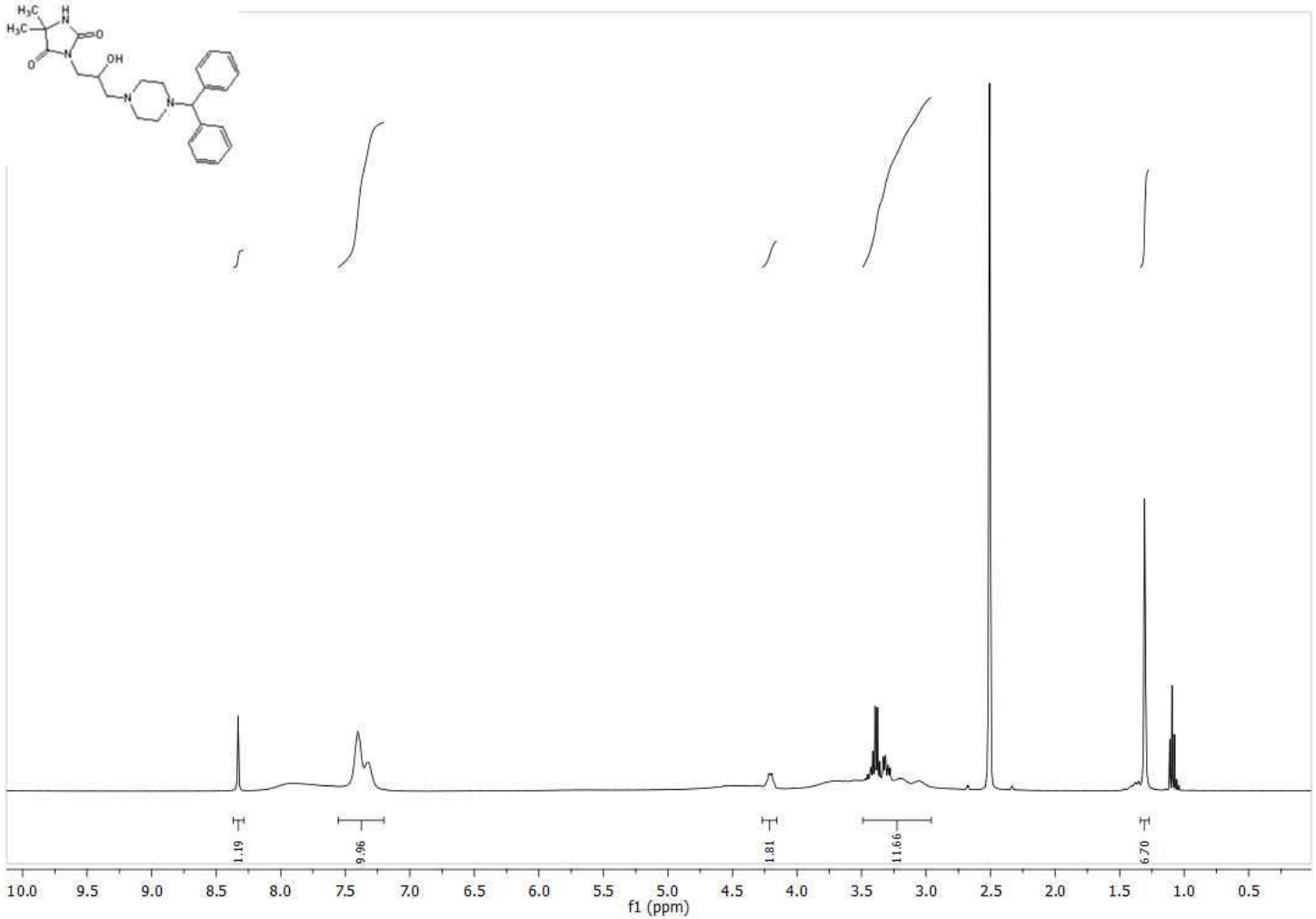

^{13}C NMR. 300 MHz. DMSO

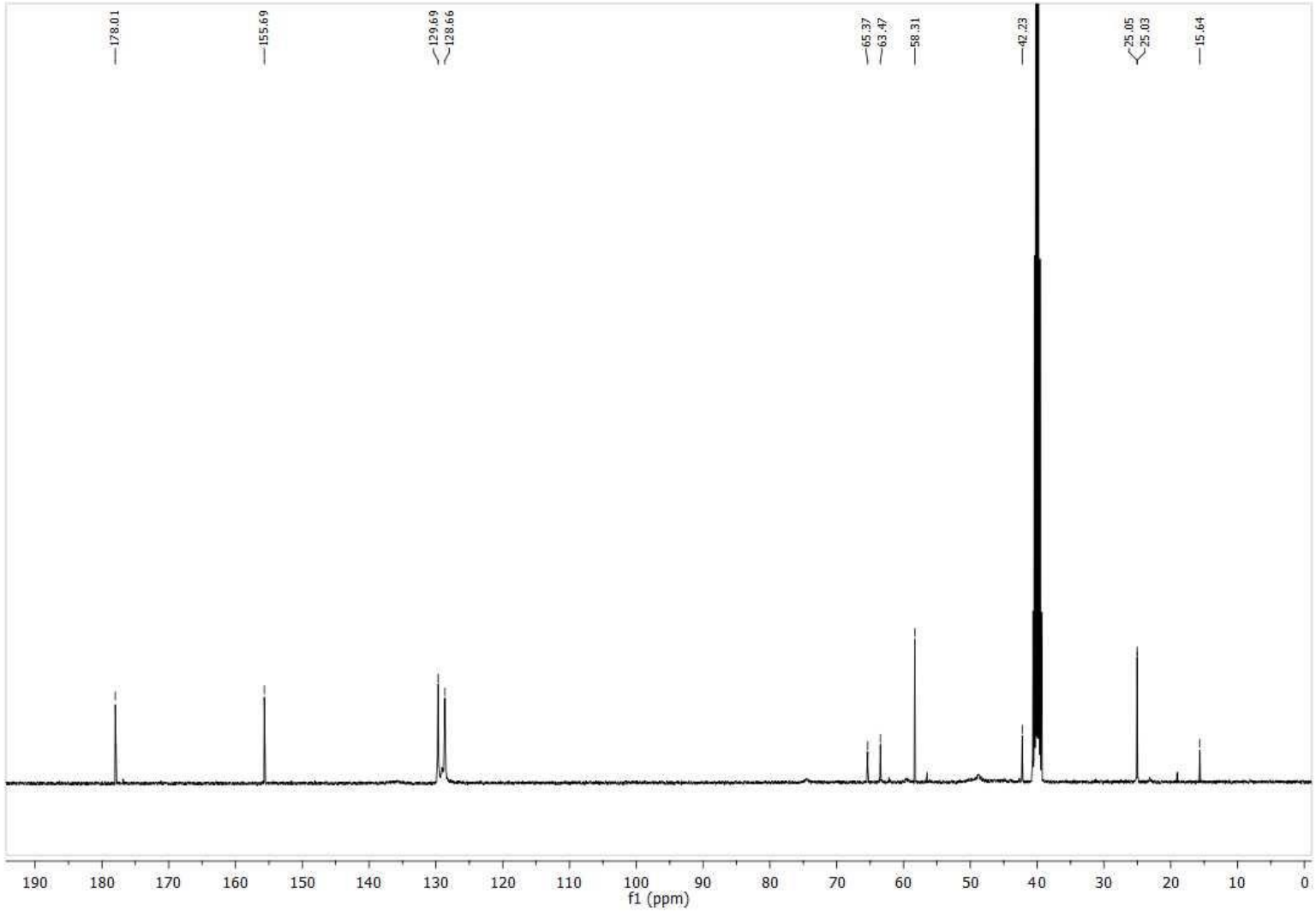

5-(4-fluorophenyl)-3-[2-hydroxy-3-(1,2,3,4-tetrahydroisoquinolin-2-yl)propyl]-5-methylimidazolidine-2,4-dione **(18)**

^{1}H NMR. 300 MHz. DMSO

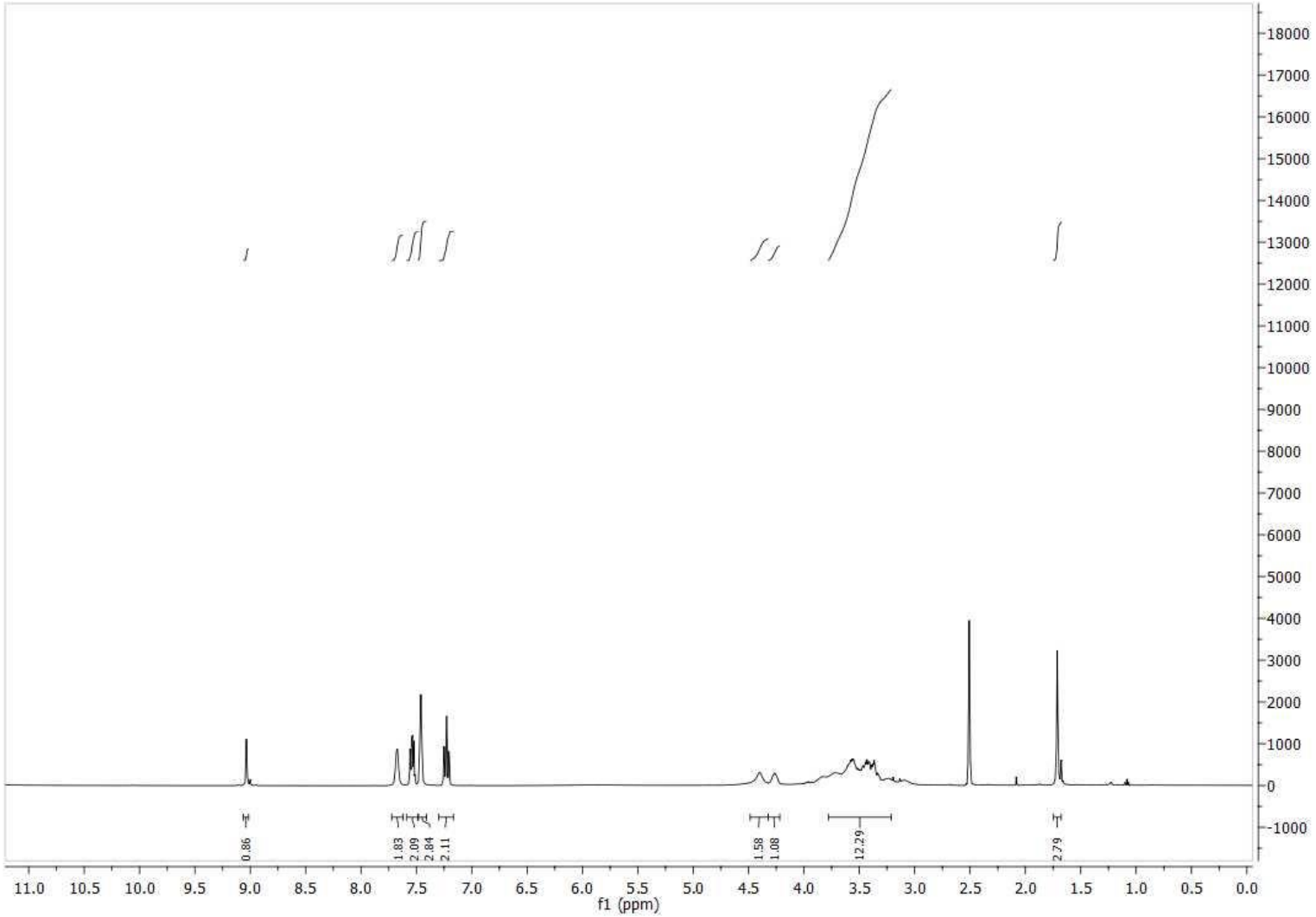

^{13}C NMR. 300 MHz. DMSO

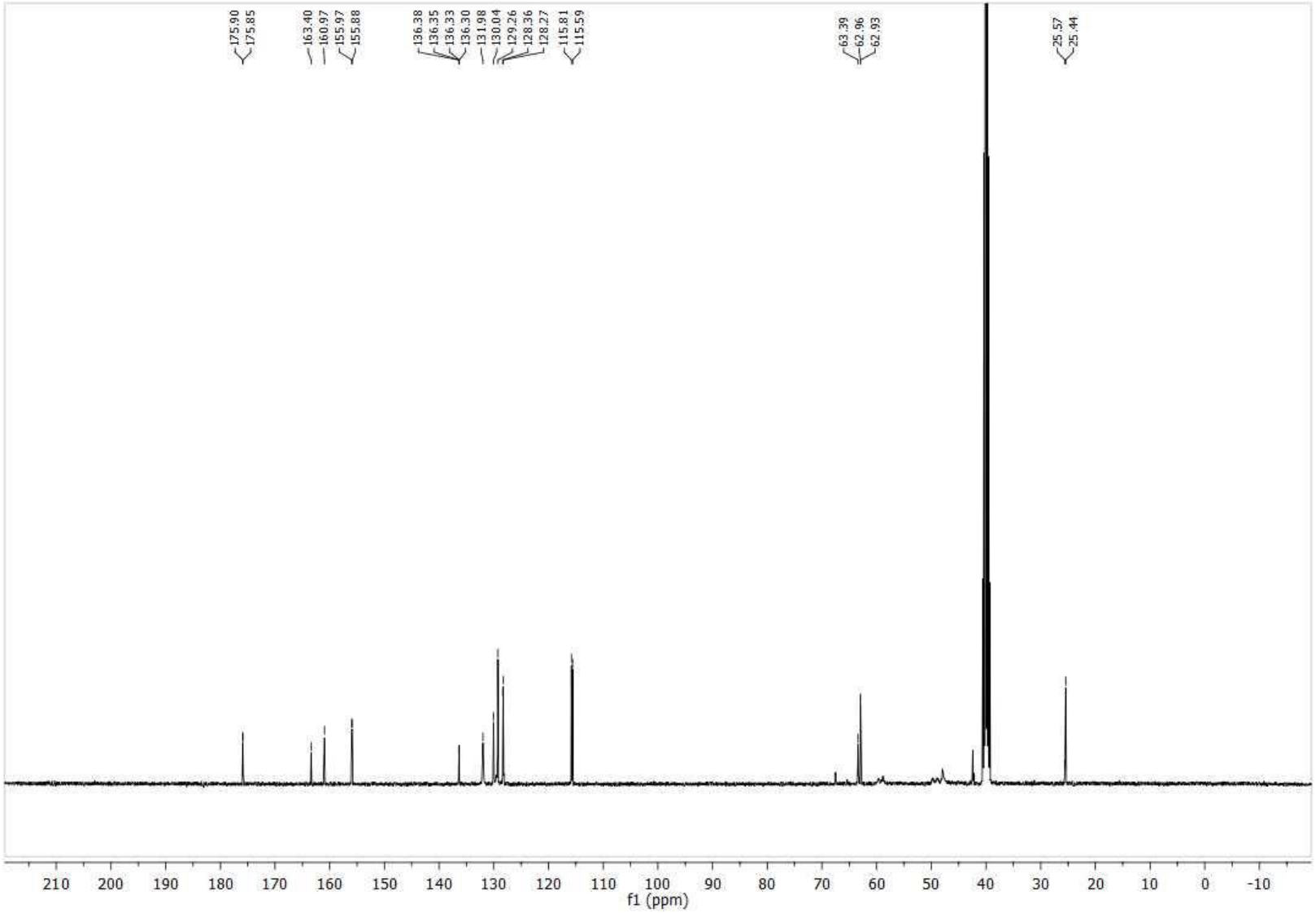

Characteristics of intermediates 23 and 24

*5-methyl-5-(naphthalen-1-yl)-3-(oxiran-2-ylmethyl)imidazolidine-2,4-dione (***23)**
White solid. Yield 35%. LC/MS±: t_R=5.06, (ESI) m/z [M+H] 297.13. ^{1}H NMR δ (ppm): 9.01 (s, 1H, N^{1}H), 8.03 (s, 1H, Ar), 7.95-7.91 (m, 3H, Ar), 7.65 – 7.59 (m, 1H, Ar), 7.59 – 7.51 (m, 2H, Ar), 4.03-3.97 (m, 1H, CH), 3.60-3.59 (m, 2H, CH_2), 2.70 (m, 1H, CH_{2a}), 2.44 (m, 1H, CH_{2b}), 1.78 (s, 3H, CH_3).

5-methyl-5-(naphthalen-2-yl)-3-(oxiran-2-ylmethyl)imidazolidine-2,4-dione (**24**)
White solid. Yield 43%. LC/MS±: t_R=5.32, (ESI) m/z [M+H] 297.13. ^{1}H NMR δ (ppm): 8.85 (s, 1H, N^{1}H) 8.02 – 7.96 (m, 2H, Ar), 7.77-7.75 (m, 1H, Ar), 7.57-7.53 (m, 4H, Ar), 4.20 – 4.11 (m, 1H, CH), 3.31 – 3.20 (m, 6H, CH_2), 2.83 (m, 1H, CH_{2a}), 2.64 – 2.57 (m, 1H, CH_{2b}), 1.93 (s, 3H, CH_3).